THE JOURNAL OF PHYSICAL CHEMISTRY C
A JOURNAL OF THE AMERICAN CHEMICAL SOCIETY

pubs.acs.org/JPCC

Article

An Oxygen-Centric View of the Structure of Alkali and Alkaline-Earth Metaphosphate Glasses: Results from High-Resolution ^{17}O Solid State NMR Spectroscopy

Shih-Yi Chuang, Ivan Hung, Zhehong Gan, and Sabyasachi Sen*

Cite This: *J. Phys. Chem. C* 2026, 130, 6243−6259

Read Online

ACCESS | Metrics & More | Article Recommendations

ABSTRACT: The physicochemical properties of phosphate glasses are strongly influenced by the modifier cation−oxygen bonding interaction and the spatial distribution of modifier cations, yet direct experimental insight into these structural-chemical aspects remains limited. In this work, we present a comprehensive multinuclear (^{31}P and ^{17}O) NMR study of single- and mixed-modifier metaphosphate glasses containing alkali (Li, Na, Rb) and alkaline-earth (Mg, Ca, Ba) cations with identical nominal network connectivity. The ^{31}P magic-angle-spinning (MAS) NMR spectra confirm that the network structure of these glasses is dominated by Q^2 phosphate units, while ^{17}O MAS and triple-quantum MAS (3QMAS) NMR provide an oxygen-centric view of bridging (BO) and nonbridging oxygen (NBO) environments and elucidate their interactions with the modifier cations. A relationship between the ^{17}O quadrupolar asymmetry parameter and the P−O−P bond angle is established using *ab initio* calculations, enabling extraction of the bond-angle distribution (BAD) directly from experimental ^{17}O 3QMAS NMR data. These distributions show increased disorder in the P−O−P BAD with increasing modifier field strength, consistent with enhanced chain folding/coiling effects. Analysis of ^{17}O 3QMAS isotropic line shapes in single- vs mixed- modifier glasses in conjunction with bond-valence considerations indicates that the mixing between alkali and alkaline-earth cations are more uniform, while that between dissimilar alkali cations is more random. Such cation mixing behavior appears to be controlled by the structural preference to maximize a uniform spatial charge distribution and to play a key role in controlling the dependence of the glass transition and ionic transport behavior on the modifier compositional makeup.

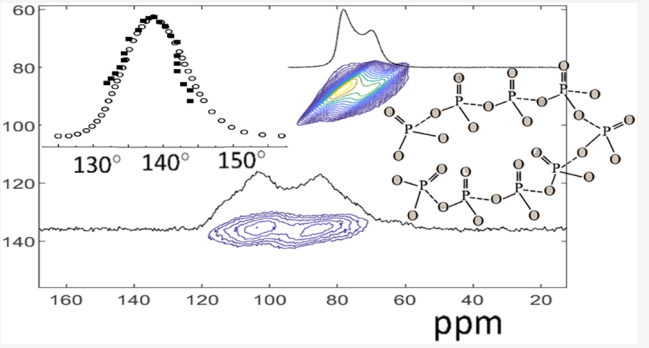

1. INTRODUCTION

Phosphate glasses constitute an important family of oxide network glass-forming systems with relatively unique properties including low melting point and glass transition temperature T_g, high coefficient of thermal expansion, good UV transparency, relatively high solubility of rare earth and other high-field strength cations, strong bioactivity and in some cases fast ionic mobility.[1−9] These unique characteristics enable their applications in the areas of glass-to-metal sealing, laser host medium, nuclear waste encapsulation, biomedicine and solid electrolytes. The atomic structure of these glasses has therefore been investigated using a wide variety of diffraction and spectroscopic techniques as well as molecular dynamics simulations to build predictive models of structure−property relationships.[10−20]

Nuclear magnetic resonance (NMR) spectroscopy, being an element specific technique sensitive to short and intermediate range order, played an important role in this regard as ^{31}P is a highly sensitive NMR-active spin-1/2 nuclide with 100% natural abundance. High-resolution ^{31}P NMR spectra for phosphate glasses can be obtained relatively readily by magic-angle-spinning (MAS) at moderate magnetic fields (e.g., 9.4 or 11.7 T) and spinning speeds (e.g., 10−15 kHz). Such spectra can yield short-range information on the phosphate Q^n speciation where n denotes the number of bridging oxygen atoms on a PO_4 tetrahedron.[10−13] Moreover, two-dimensional (2D) NMR spectroscopic techniques can also yield intermediate-range structural information in terms of the connectivity between the constituent Q^n species.[14,15] On the other hand, X-ray and neutron diffraction techniques have been employed in the past to investigate the local bonding environment of the modifier cations M.[16−18] The results from such studies were used to hypothesize how, with increasing

Received: February 24, 2026
Revised: April 10, 2026
Accepted: April 10, 2026
Published: April 20, 2026

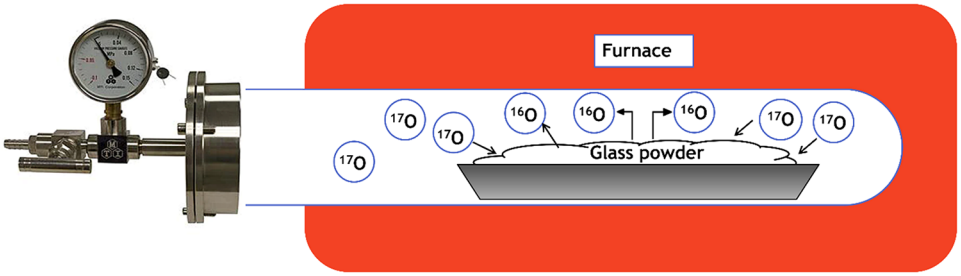

Figure 1. Schematic of experimental setup for solid ↔ gas oxygen isotope exchange.

modifier content, the connectivity established between the M−O polyhedra may provide additional rigidity to the phosphate network and can explain the nonmonotonic compositional variation of molar volume and the glass transition temperature T_g. Additionally, the average spatial distribution of alkali cations and the degree of mixing between unlike alkalis have been studied in various oxide and chalcogenide glasses using spin−echo decay NMR spectroscopy and its heteronuclear variants such as the rotational echo double resonance and spin−echo double resonance techniques.[21−27]

However, systematic experimental studies of the local spatial distribution of M cations and their relative affinity for nonbridging oxygen (NBO) vs bridging oxygen (BO) atoms can be done most directly using ^{17}O NMR spectroscopy, and such studies have remained rather limited in literature even in the case of simple phosphate crystals and glasses. A case in point is the relative affinity of alkali atoms for bonding with NBO and BO atoms in binary alkali phosphate crystals. For example, all Na atoms are solely bonded to NBO atoms in $NaPO_3$, while BO atoms participate in the coordination shells of Na atoms in $Na_5P_3O_{10}$ and in $Na_4P_2O_7$.[28−31] A similar situation is observed in the case of KPO_3 and $AgK(PO_3)_2$, where the K atoms are found to have significant bonding interaction with BO atoms in their nearest-neighbor coordination shells.[32,33] Such structural aspects are not only important in understanding static properties such as molar volume in terms of atomic packing, but also dynamic properties such as long-range ionic transport in these glasses. The spatial distribution of M cations is also at the heart of the fundamental models of glass structure such as the continuous random network (CRN) model and the modified random network (MRN) model.[34−36] As opposed to CRN that hypothesizes a relatively random spatial distribution of the M cations, the MRN proposes a preferential clustering of these cations in channels decorated by NBO atoms. Therefore, the MRN model suggests sharing of NBOs between M−O polyhedra and minimal bonding interaction between the BO atoms and the M cations in the glass structure. The existence of these ion channels in a MRN also has consequences for the diffusivity of the M cations and hence, on the ionic conductivity of glasses.

Analyses of temperature-dependent viscosity data, $\eta(T)$, for alkali phosphate liquids containing ≥50 mol % P_2O_5 reported in the literature demonstrate that the fragility index.

$$m = \left.\frac{d[\log \eta(T)]}{d(T_g/T)}\right|_{T=T_g}$$

as well as T_g are highly sensitive to the structural connectivity of the phosphate network.[37,38] As the connectivity increases with progressive addition of P_2O_5, the PO_4 groups become increasingly cross-linked, leading to a corresponding decrease in m and increase in T_g. However, recent studies have shown that even in metaphosphate liquids (50 mol % P_2O_5) with identical nominal network connectivity controlled by the predominant presence of Q^2 units, m and T_g can vary over a wide range depending on the field strength of the M cation.[39,40] Metaphosphates containing high field strength M cations, such as the alkaline-earths, exhibit relatively low m and high T_g, whereas those modified by low field strength M cations such as alkalis display significantly higher m and lower T_g values. This behavior has been attributed to the variations in the extent and strength of effective cross-linking of phosphate chains in metaphosphates by the M−O polyhedra, which increases with increasing field strength of the M cations.[39]

These hypothesized structural and bonding scenarios can be directly interrogated by building an oxygen-centric view of the phosphate glass structure using high-resolution ^{17}O NMR spectroscopy. This type of studies was pioneered in the literature for silicate glasses by Stebbins and co-workers.[41−45] Here we report the results of such a structural study of binary alkali (Li, Na, Rb) and alkaline-earth (Ca, Mg, Ba) phosphate glasses with nominal metaphosphate composition, i.e., with similar network connectivity, where the M cation field strength was systematically varied. We have utilized ^{31}P and ^{17}O NMR spectroscopy to investigate the nature of the BO and NBO environments, the P−O−P bond angle distribution (BAD) and the M−O bonding interaction as a function of the nature of the modifier ions in these single-modifier glasses. Furthermore, ^{17}O NMR is employed to probe the spatial distribution and mixing of modifier cations in mixed-modifier metaphosphate glasses and their effect on the compositional variation of their physical properties.

2. EXPERIMENTAL DETAILS

2.1. Sample Preparation

A series of single-modifier metaphosphate glasses of compositions $NaPO_3$, $LiPO_3$, $RbPO_3$, $Mg(PO_3)_2$, $Ca(PO_3)_2$, and $Ba(PO_3)_2$ and mixed-modifier metaphosphate glasses of compositions $Li_{0.5}Rb_{0.5}PO_3$, $Na_{0.5}Li_{0.5}PO_3$, $(NaPO_3)_{0.5}(Mg_{0.5}PO_3)_{0.5}$, $(NaPO_3)_{0.5}(Ca_{0.5}PO_3)_{0.5}$, and $(NaPO_3)_{0.5}(Ba_{0.5}PO_3)_{0.5}$ were prepared by the conventional melt-quenching method. The single-modifier metaphosphate glasses were prepared using reagent grade $NH_4H_2PO_4$ (99.9%, Arcos Organics), Na_2CO_3 (99.99%, Alfa Aesar), Li_2CO_3 (99.999%, Alfa Aesar), Rb_2CO_3 (99%, Thermo Scientific), $MgCO_3$ (99%, Sigma-Aldrich), $CaCO_3$ (ACS, Sigma-Aldrich), and $BaCO_3$ (99.95%, Alfa Aesar). Stoichiometric amounts of these chemicals were mixed, taken in silica crucibles and calcined at 450 °C for 48 h to remove H_2O, NH_3, and CO_2. The batch was then transferred to a platinum crucible and melted in air at temperatures ranging between 1000 and 1300 °C for 2 h followed by quenching on a graphite plate. The mixed-modifier metaphosphate glasses were made by mixing the end member single-modifier glasses in a platinum crucible followed by

https://doi.org/10.1021/acs.jpcc.6c01260
J. Phys. Chem. C 2026, 130, 6243−6259

melting at 1000 °C for 1 h and subsequently quenching on a graphite plate.

The ^{17}O-enriched metaphosphate glasses were prepared from unenriched glass samples using a gas ↔ solid exchange method. The unenriched metaphosphate glasses were crushed into powder, taken on a platinum foil and loaded onto an alumina boat, which was then placed in a silica glass tube fitted to a clamshell furnace (Figure 1). The glass tube was sealed with a vacuum flange and pumped down to 10^{-5} atm, then backfilled with dry 70% ^{17}O enriched gas (Nukem isotopes, Germany) to 1 atm at room temperature. The tube was then heated to a temperature where the viscosity of the supercooled liquid reached a value of ∼10^2 Pa·s and held isothermally at that temperature for 4 days to promote exchange of oxygen isotope between the supercooled liquid and the gas phase (Figure 1) before cooling down back to room temperature. These temperatures, where the isotope exchange was performed, are listed in Table 1. All samples were found to be partially to completely devitrified after the exchange. Therefore, these isotope-enriched samples were transferred to a platinum crucible and remelted for 30 min to restore the glassy state and to remove any potential compositional heterogeneity formed during the exchange, followed by quenching on a graphite plate.

Table 1. Temperatures Used for Gas ↔ Solid Exchange in the Synthesis of Various ^{17}O-Enriched Metaphosphate Glasses

glass composition	exchange temperature (°C)
$NaPO_3$	600
$LiPO_3$	650
$RbPO_3$	550
$Mg(PO_3)_2$	1050
$Ca(PO_3)_2$	1000
$Ba(PO_3)_2$	800

2.2. NMR Spectroscopy

2.2.1. ^{31}P NMR Spectroscopy. The ^{31}P magic-angle-spinning (MAS) NMR spectra of all glasses were collected using a Bruker Avance 500 spectrometer operating at a ^{31}P Larmor frequency of 202.4 MHz (magnetic field of 11.7 T). Crushed glass samples were taken in 4 mm ZrO_2 rotors and were spun at 15 kHz using a Bruker triple-resonance MAS probe. The one-pulse ^{31}P MAS NMR spectra were acquired using a $\pi/6$ pulse (0.84 μs) and a recycle delay of 60 s. A total of 64 free induction decays were averaged and Fourier transformed to obtain each spectrum. All ^{31}P spectra were externally referenced to Na_2HPO_4 with δ_{iso} at 4.6 ppm. One-pulse ^{31}P MAS NMR spectra were also collected on select glass compositions with a longer recycle delay of 300 s to ensure that a shorter delay of 60 s was sufficient to obtain quantitative spectra. All simulations and analysis of ^{31}P and ^{17}O NMR spectral line shapes were carried out using the software DMFit.[46] The three principal components of the ^{31}P NMR chemical shift tensor δ_{xx}, δ_{yy} and δ_{zz} were recast into the isotropic shift δ_{iso}, and the magnitude Δ and asymmetry η of the chemical shift anisotropy (CSA) following the Haeberlen convention[47] $|\delta_{zz} - \delta_{iso}| \geq |\delta_{xx} - \delta_{iso}| \geq |\delta_{yy} - \delta_{iso}|$, with

$$\delta_{iso} = \frac{1}{3}(\delta_{zz} + \delta_{xx} + \delta_{yy}) \quad (1)$$

$$\Delta = \delta_{zz} - \delta_{iso} \quad (2)$$

$$\eta = \frac{\delta_{yy} - \delta_{xx}}{\Delta} \quad (3)$$

2.2.2. ^{17}O NMR Spectroscopy. A low-field ^{17}O MAS NMR spectrum of the ^{17}O-enriched $NaPO_3$ glass was collected using a Bruker Avance 500 spectrometer operating at a ^{17}O Larmor frequency of 67.8 MHz (11.7T). Crushed $NaPO_3$ glass was taken in a 4 mm ZrO_2 rotor and was spun at 10 kHz using a Bruker triple-resonance MAS probe. The one-pulse ^{17}O MAS NMR spectrum was acquired using a solids $\pi/6$ pulse (0.6 μs) and a recycle delay of 0.5 s. A total of 64 free induction decays were averaged and Fourier transformed to obtain the spectrum, which was externally referenced to H_2O with δ_{iso} at 0 ppm.

The ^{17}O triple-quantum MAS (3QMAS) NMR spectra of all ^{17}O-enriched glasses were acquired at the National High Magnetic Field Laboratory (NHMFL, Tallahassee, Florida) using a Bruker Avance 850 NEO console operating at a ^{17}O Larmor frequency of 115.3 MHz (B_0 = 20 T) and a Low-E 3.2 mm HX MAS probe designed and constructed at the NHMFL. Crushed glass samples were packed into 3.2 mm ZrO_2 rotors and spun at 16 kHz. A shifted-echo SPAM MQMAS pulse sequence was used.[48−50] Pulses of 3 and 1 μs were used for excitation and conversion of 3Q coherence with a rf amplitude of ∼110 kHz. The indirect spectral window was rotor-synchronized by incrementing the t_1 delay by the rotor period, 62.5 μs. The recycle delay, number of averaged transients, number of complex points acquired in the indirect dimension, and total experiment time for each sample are listed in Table 2. The whole-echo ^{17}O 3QMAS spectra were processed by Fourier transformation of the direct dimension, followed by shearing of the indirect dimension using t_1-dependent first-order phase correction,[51] and then Fourier transformation of the direct dimension.

Table 2. Experimental Conditions Used for Acquisition of ^{17}O 3QMAS NMR Spectra of Various Single- and Mixed-Modifier Alkali and Alkaline-Earth Metaphosphate Glasses

composition	recycle delay (s)	transients	t_1 points	experiment time (h)
$NaPO_3$	0.7	288	48	2.7
$LiPO_3$	0.7	2112	48	19.7
$RbPO_3$	0.7	1440	20	5.6
$Mg(PO_3)_2$	0.7	960	24	4.5
$Ca(PO_3)_2$	0.7	384	40	3.0
$Ba(PO_3)_2$	0.2	13,920	24	18.6
$NaMg_{0.5}(PO_3)_2$	0.7	1056	48	9.9
$NaCa_{0.5}(PO_3)_2$	0.7	576	20	2.2
$NaBa_{0.5}(PO_3)_2$	0.2	2880	96	15.4
$NaLi(PO_3)_2$	1.0	288	40	3.2
$LiRb(PO_3)_2$	0.7	1920	20	7.5

2.3. Calculation of ^{17}O NMR Quadrupolar Parameters Using Density Functional Theory

The ^{17}O NMR quadrupolar coupling constant C_Q and the asymmetry parameter of the electric field gradient (EFG) tensor η are calculated in select crystalline phosphate compounds ($Na_3P_3O_9$, $Na_4P_2O_7$, $Na_5P_3O_{10}$, $Ba(PO_3)_2$, $Ba_2P_2O_7$, $LiPO_3$, $Mg_2P_2O_7$, $Na_2Ca(PO_3)_4$, and $NaBa(PO_3)_3$) using the gauge-including projector augmented wave (GIPAW) method based on density functional theory (DFT)[52−54] to establish a relationship between C_Q, η and the P−O−P bond angle θ. The GIPAW method allows the reconstruction of the all-electron magnetic response within a pseudopotential formalism well suited for extended systems with periodic boundary conditions. The atom positions in the phosphate crystal structures as reported in the literature[55−61] were first optimized using DFT-based geometry optimization prior to the calculation of the NMR parameters. All calculations were carried out using the code CASTEP-NMR (Biovia Inc.) within the generalized gradient approximation with Perdew−Burke−Ernzerhof (PBE) XC functionals using on-the-fly generated ultrasoft pseudopotentials and plane wave basis sets with an energy cutoff of 610 eV, where the total energy converged within 10^{-7} eV/atom. The Brillouin zone was sampled using the Monkhorst−Pack scheme and a 4 × 4 × 4 k-point grid. The EFG tensor was calculated from the second spatial derivative of the electrostatic potential associated with the charge density in the crystal. Diagonalization of this second rank tensor yields the principal components $V_{zz} \geq V_{yy} \geq V_{xx}$, which can be used to calculate C_Q and η following the relations

https://doi.org/10.1021/acs.jpcc.6c01260
J. Phys. Chem. C 2026, 130, 6243−6259

$$C_Q = eQ|V_{zz}|/h \quad (4)$$

$$\eta = \frac{V_{xx} - V_{yy}}{V_{zz}} \quad (5)$$

where e is the electronic charge, h is Planck's constant, and Q is the quadrupole moment of ^{17}O (−25.58 mB). The results of these calculations are listed in Table 3. The calculated ^{17}O C_Q and η agree well with the experimentally measured values that have been reported in the literature for a limited set of phosphate compounds (Table 3).[55,62]

Table 3. ^{17}O Quadrupolar Parameters Calculated by DFT for BO Sites in Geometry Optimized Structures of Select Phosphate Compounds[a]

compound	P−O−P angle (°)	C_Q (MHz)	η
$Ba(PO_3)_2$	119.70	7.22	0.71
	144.00	8.54	0.27
$Na_5P_3O_{10}$	121.80	7.33	0.66
$BaNa(PO_3)_3$	125.80	7.48	0.64
	126.60	7.53	0.61
	130.60	7.99	0.54
$Na_3P_3O_9$	126.00	7.40 (~7.0)	0.65 (0.60 ± 0.05)
	127.00	7.60	0.60
$Na_4P_2O_7$	127.13	7.10 (7.3)	0.62 (0.55 ± 0.05)
$LiPO_3$	133.00	8.10	0.46
	138.00	8.12	0.40
	140.00	8.47	0.38
	142.00	8.55	0.37
$Ba_2P_2O_7$	133.30	7.80	0.42
$Na_2Ca(PO_3)_4$	135.00	7.96	0.37
$Mg_2P_2O_7$	143.40	8.44	0.30

[a]Values in parentheses correspond to experimentally determined C_Q and η for select compounds, reported in literature.[55,62]

3. RESULTS AND DISCUSSION

3.1. Single-Modifier Metaphosphate Glasses

The ^{31}P MAS NMR spectra of all single-modifier (SM) metaphosphate glasses studied here are dominated by the resonance characteristic of the Q^2 phosphate unit, confirming that the structural network of these glasses is primarily composed of metaphosphate chains (Figure 2). Minor contribution from Q^1 species is also detected in some compositions as a weak resonance located downfield, with up to ~8% of P being present in the form of Q^1 (Figure 2). Such small fraction of Q^1 species does not significantly affect the average connectivity of the phosphate network. On the other hand, no significant contribution from Q^3 species is observed in these ^{31}P MAS NMR spectra. Therefore, the presence of Q^1 is not a result of Q-species disproportionation but likely reflects slight deviation of the glass composition from the metaphosphate stoichiometry with a modifier excess of up to 1 mol % and/or the presence of a small amount of residual water in the form of hydroxyl group that leads to chain termination effects. The ^{31}P NMR parameters δ_{iso}, Δ, and η for the Q^2 species and δ_{iso} for the Q^1 species, as obtained from the simulation of the corresponding center band and spinning sidebands in the ^{31}P MAS NMR spectra are reported in Table 4. The signal from the Q^1 species in these ^{31}P MAS NMR spectra was found to be too weak to obtain reliable values of Δ and η from the ^{31}P MAS spectra.

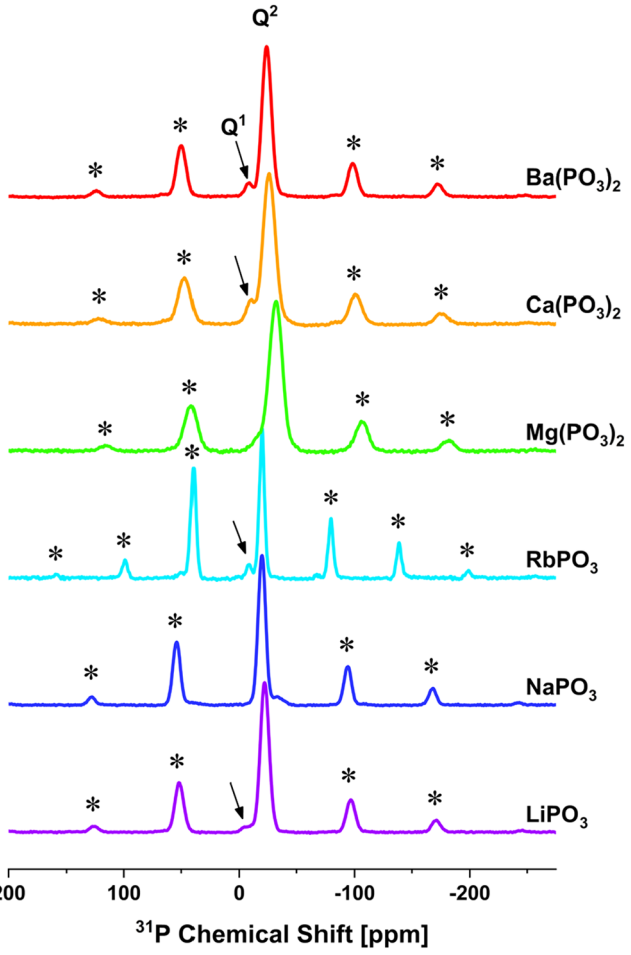

Figure 2. ^{31}P MAS NMR spectra of single-modifier metaphosphate glasses. Glass compositions are denoted alongside each spectrum. Asterisks denote spinning sidebands.

Table 4. ^{31}P NMR Parameters for Constituent Q Species in Various Single-Modifier Alkali and Alkaline-Earth Metaphosphate Glasses[a]

glass composition	site	δ_{iso} (±0.5 ppm)	Δ (±5 ppm)	η (±0.05)
$NaPO_3$	Q^2	−19.8	−146	0.42
$LiPO_3$	Q^1	−7.0	N.D.	N.D.
	Q^2	−22.3	−131	0.45
$RbPO_3$	Q^1	−9.2	N.D.	N.D.
	Q^2	−19.8	−148	0.42
$Mg(PO_3)_2$	Q^1	−16.0	N.D.	N.D.
	Q^2	−32.0	−131	0.44
$Ca(PO_3)_2$	Q^1	−9.6	N.D.	N.D.
	Q^2	−26.2	−130	0.38
$Ba(PO_3)_2$	Q^1	−8.3	N.D.	N.D.
	Q^2	−23.9	−134	0.45

[a]N.D. = not determined.

These ^{31}P NMR parameters are in good agreement with those reported in previous studies on glasses of similar composition in the literature. Here we note that previous ^{31}P NMR studies of metaphosphate glasses indicated that the ^{31}P δ_{iso} decreased, i.e., its shielding increased, and the line width (FWHM) increased nearly linearly with increasing potential Z/a of the M cation, where Z and a are its charge and radius.[63−65] This trend in ^{31}P δ_{iso} was explained to be due to a decrease in

https://doi.org/10.1021/acs.jpcc.6c01260
J. Phys. Chem. C 2026, 130, 6243−6259

the covalency of the P−O bond in the presence of strongly electronegative M cations, which decreases the paramagnetic deshielding of the ^{31}P nuclide. These authors also noted that the correlation became worse when the cation field strength Z/a^2 was considered instead of its potential. On the other hand, the trend in FWHM was related to a distribution in P−O bond distance and/or P−O−P bond angle.[65] Here we show in Figure 3 that the ^{31}P δ_{iso} of the Q^2 species in the

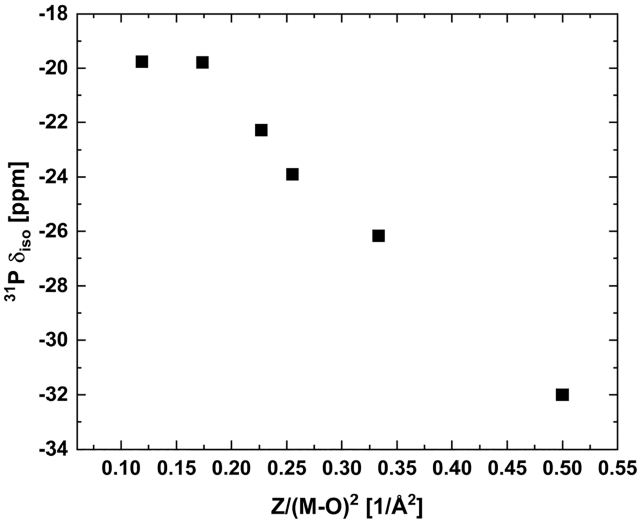

Figure 3. Variation of ^{31}P isotropic chemical shift with field strength of modifier cations. Error bars are within the size of symbols.

metaphosphate glasses used in the present study indeed systematically decreases with increasing field strength of the alkali or alkaline-earth M cation, where the field strength of a cation M is defined as the ratio Z/r^2 with r being the typical M−O bond distance in these glasses, as determined by previous diffraction studies.[16−18]

At the outset of presenting the ^{17}O NMR results on these glasses, we note that besides the low natural abundance of the ^{17}O nuclide, which can be circumvented by enriching the samples with ^{17}O isotope, its NMR spectroscopy is further complicated by its low sensitivity and large quadrupolar broadening.[55,66,67] Although MAS can average the first order quadrupolar broadening effects, the second order broadening effects for the BO and NBO sites in phosphates can be substantial.[55,66,67] This situation is demonstrated in Figure 4 where the ^{17}O MAS spectrum of the $NaPO_3$ glass collected in this study at a magnetic field of 11.7 T shows strong overlap between the two constituent resonances. Simulation of this central-transition line shape (Figure 4) yields the following NMR parameters for these two resonances: δ_{iso} ∼ 85 ppm and ∼125 ppm, quadrupolar coupling constant C_Q of ∼4.8 MHz and ∼7.7 MHz and quadrupolar asymmetry parameter η of 0.30 and 0.60. These two resonances can be readily assigned to the NBO and BO sites, respectively, on the basis of their relative abundance of 2:1, as expected for a metaphosphate composition. These ^{17}O NMR parameters for the NBO and BO sites are also consistent with those reported in a previous study by Zeyer et al.[66]

Such challenges with the sensitivity and quadrupolar broadening in ^{17}O NMR can, however, be efficiently untangled by performing multiple-quantum MAS (MQMAS) NMR spectroscopy at higher magnetic fields of ≥20 T.[55] The

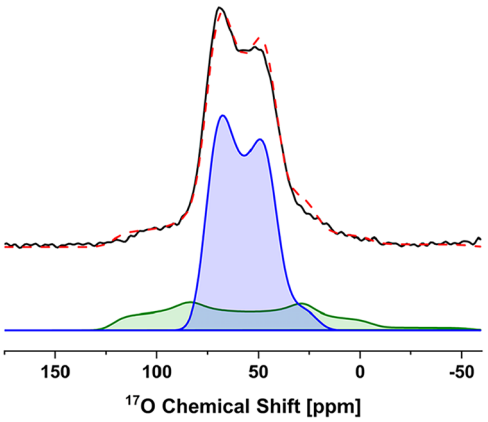

Figure 4. Experimental (black solid line) and simulated (red dashed line) ^{17}O MAS NMR of $NaPO_3$ glass obtained at 11.7 T. Individual simulation components are shown as blue and green shaded line shapes corresponding, respectively, to NBO and BO sites. Simulation components are offset for clarity.

MQMAS experiment is a two-dimensional NMR spectroscopic technique that relies on mixing single- and multiple-quantum coherences to generate an isotropic spectrum free of second-order quadrupolar broadening effects in the indirect dimension, which is correlated with the single-quantum MAS central-transition spectrum in the direct dimension. In this case the spectrum in the isotropic dimension is only broadened by the distributions of the chemical and isotropic quadrupolar shifts. Such spectra also allow for the study of the distributions of C_Q and η for a specific structural site in a disordered material, as a function of its δ_{iso}, i.e., its local environment.[68,69] Therefore, in the present study we focus on the application of the ^{17}O triple-quantum MAS (3QMAS) technique to study the structure of these phosphate glasses.

The ^{17}O 3QMAS spectra of the binary SM metaphosphate glasses studied here are shown in the form of contour plots in Figures 5a,b. These spectra are generally similar in the sense that they are dominated by two distinct resonances, one with a significantly higher relative intensity and smaller C_Q than the other, which can be assigned to NBO and BO sites, respectively.[55,66] These two sites are also clearly resolved in the isotropic dimension for all glasses, except for the $Ba(PO_3)_2$ glass, where the isotropic line shapes for these two sites overlap (Figure 5b). It is interesting here to note that where resolved, simulation of the spectral projection in the isotropic dimension with Gaussian line shapes yields an NBO/BO ratio of ∼3:1 instead of the expected value of 2:1 for metaphosphates. This deviation from the expected value may be due to less efficient 3QMAS excitation of the BO resonance compared to the NBO resonance, owing to the significantly larger C_Q of the former.[70] Simulation of the MAS projections of the NBO and BO signals in these 3QMAS spectra yields the δ_{iso}, C_Q and η for the NBO ad BO sites in these glasses, which are listed in Table 5. The δ_{iso}, C_Q and η for the P−O−P BO sites vary over a relatively narrow ranges of 114−125 ppm, 7.4−8.1 MHz and 0.34−0.43, respectively. Such narrow ranges for the ^{17}O NMR parameters in a wide range of glass compositions is not surprising considering the P−O−P oxygen environment is not significantly affected by the nature of the M cation in the structure. However, it is interesting to note that the ^{17}O δ_{iso} for the BO site systematically increases with increasing radius of the M ions (Table 5 and Figure 6), in the alkali series: from 118 ppm

https://doi.org/10.1021/acs.jpcc.6c01260
J. Phys. Chem. C 2026, 130, 6243−6259

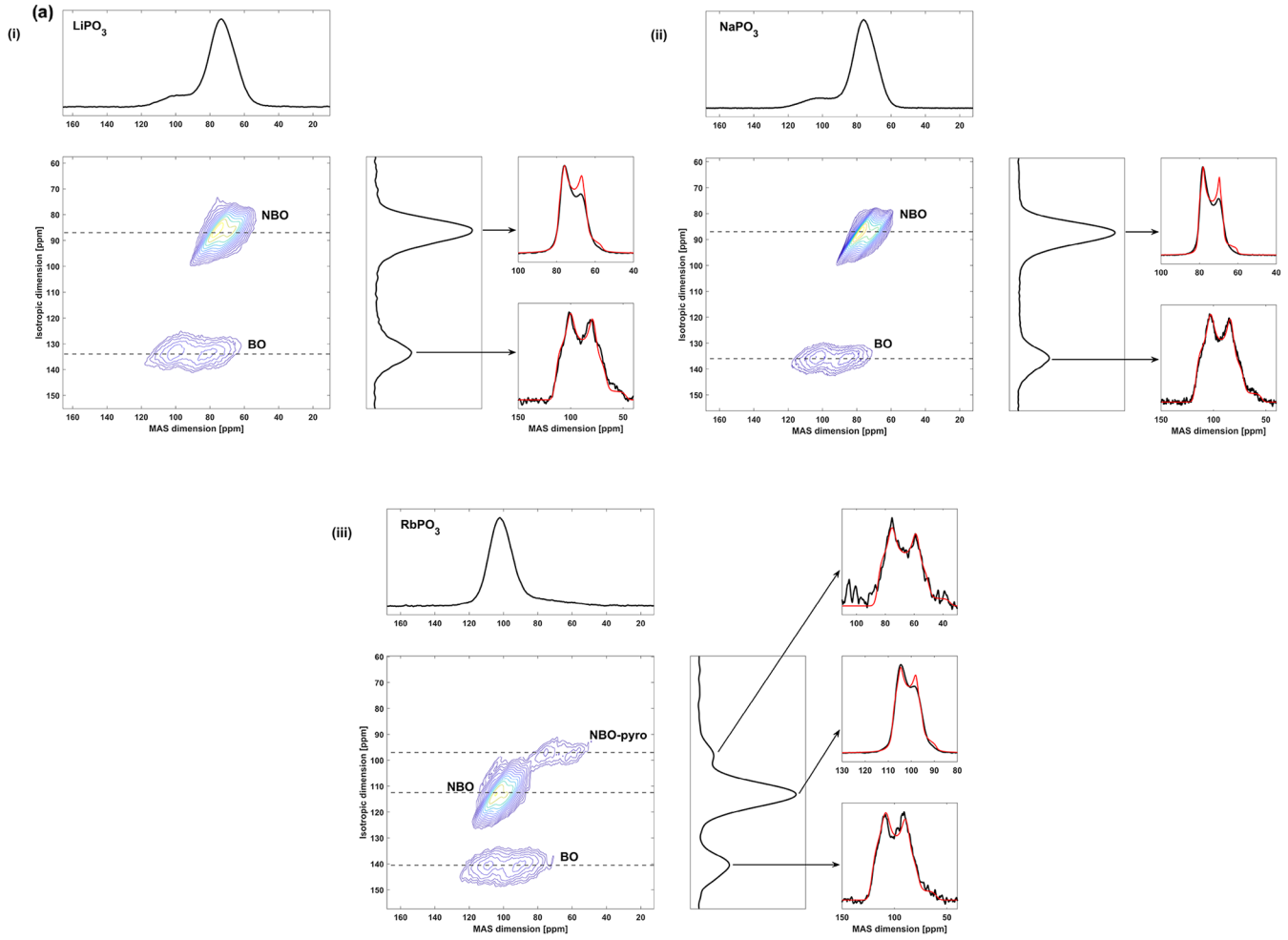

Figure 5. continued

https://doi.org/10.1021/acs.jpcc.6c01260
J. Phys. Chem. C 2026, 130, 6243−6259

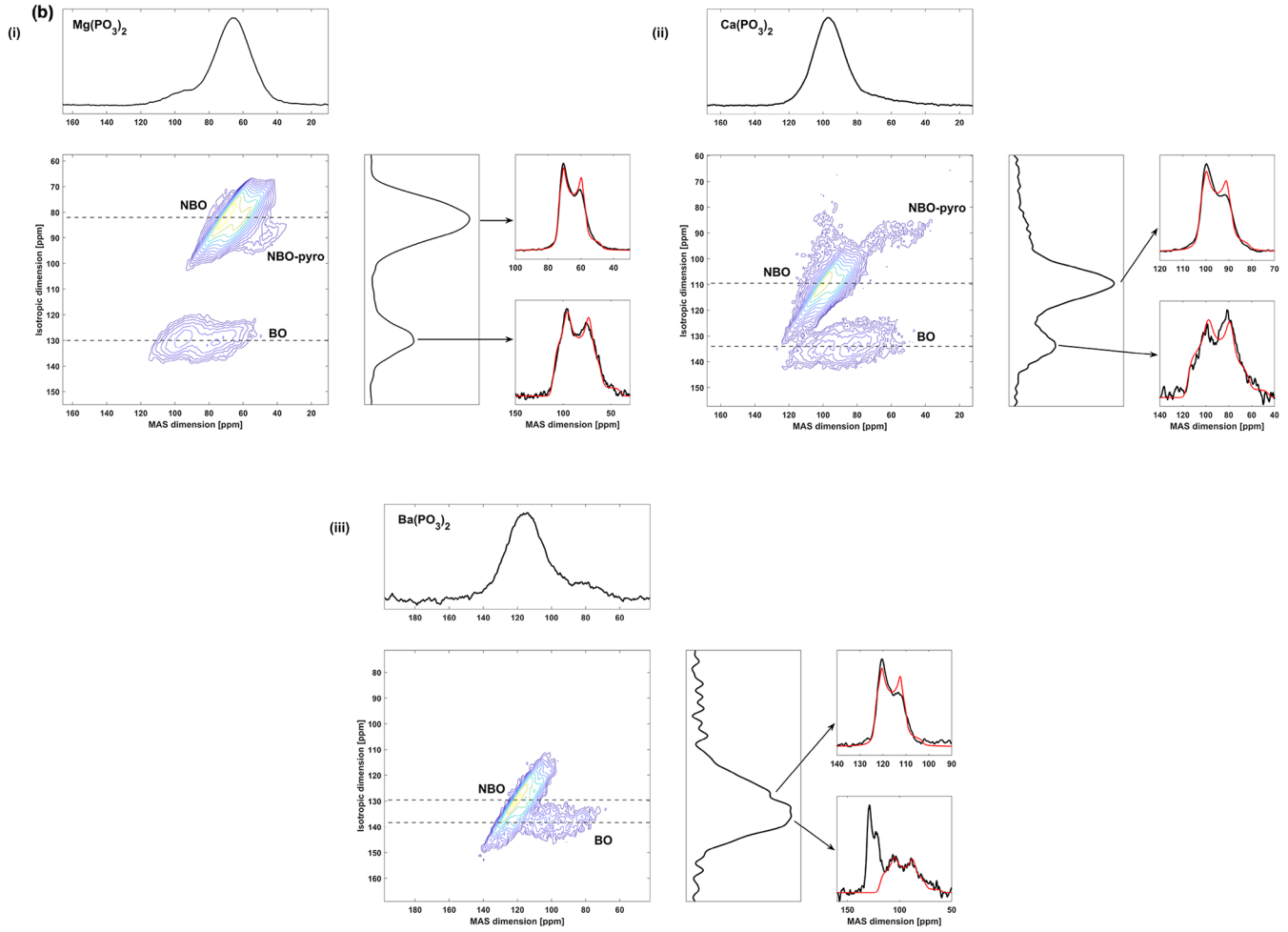

Figure 5. (a) Contour plots of ^{17}O 3QMAS NMR spectra of (i) $LiPO_3$ (top left), (ii) $NaPO_3$ (top right), and (iii) $RbPO_3$ (bottom) glasses. NBO and BO sites corresponding to the Q^2 species are denoted alongside the contours. NBO-pyro corresponds to NBO on Q^1 species. Total projections along the MAS and isotropic dimensions are shown for each spectrum. MAS slices (black line) at the isotropic peak positions and corresponding simulated line shapes (red line) are shown on the extreme right panels. (b) Contour plots of ^{17}O 3QMAS NMR spectra of (i) $Mg(PO_3)_2$ (top left), (ii) $Ca(PO_3)_2$ (top right), and (iii) $Ba(PO_3)_2$ (bottom) glasses. NBO and BO sites corresponding to the Q^2 species are denoted alongside the contours. NBO-pyro corresponds to NBO on Q^1 species. Total projections along the MAS and isotropic dimensions are shown for each spectrum. MAS slices (black line) at the isotropic peak positions and corresponding simulated line shapes (red line) are shown on the extreme right panels.

for $LiPO_3$ to 125 ppm for $RbPO_3$, and in the alkaline-earth series: from 114 ppm for $Mg(PO_3)_2$ to 122 ppm for $Ba(PO_3)_2$. On the other hand, the ^{17}O δ_{iso}, C_Q, and η for the P−O−M NBO sites range between 77 and 125 ppm, 4.5−5.1 MHz and 0.20−0.27, respectively (Table 5). The ^{17}O δ_{iso} for NBO appears to show a positive correlation with the average M-NBO distance typical of phosphates, i.e., the ^{17}O nuclide in the NBO environment in these metaphosphate glasses gets progressively deshielded with increasing M−O distance (Figure 7). This correlation is similar to the trend of ^{17}O δ_{iso} for BO sites with the ionic radius of M cations in these glasses as shown in Figure 6. For example, typical Mg−O and Li−O distances in phosphates are relatively short, ∼2.0−2.1 Å, while the Ca−O distances are intermediate, ∼2.4−2.5 Å and Rb−O and Ba−O distances are significantly longer, ∼2.8−2.9 Å.[16−18,56,57,71−73] The corresponding values of ^{17}O δ_{iso} for the NBO are (see Table 5): ∼76−83 ppm, ∼105 ppm and ∼112−125 ppm, respectively. It is interesting to note that a similar trend was reported in a previous study by Turner et al. on group-II metal oxides where the ^{17}O δ_{iso} was observed to increase with increasing cation radius.[74]

Previous systematic ^{17}O NMR studies have shown that the ^{17}O C_Q for an oxygen site in oxides decreases with increasing average ionicity of the metal−oxygen bonds associated with the site.[66] This correlation is consistent with the observation of the relatively large C_Q of the P−O−P BO site, which is significantly less ionic compared to the P−O−M linkages (M = alkali, alkaline-earth), i.e., the NBO sites, with the latter being characterized by substantially lower C_Q values (Table 5). Among the phosphate glasses studied here, the NBOs in the Mg-phosphate composition shows the largest C_Q of 5.1 MHz, which may therefore suggest that the P−O−Mg linkage has the lowest ionic character.

Finally, we note that for Rb, Ca and Mg-metaphosphate glasses with a relatively high Q^1 content (6%−8%), the NBO signal shows the presence of a distinct second NBO environment (Figure 5a,b) that is characterized by a large C_Q (∼6 MHz) compared to the typical value for the majority NBO species (∼4−5 MHz). This NBO resonance, though weak, is most clearly resolved in the $RbPO_3$ glass, where a simulation of the line shape (Figure 5a) yields δ_{iso} = 80 ppm, C_Q = 6.5 MHz and η = 0.2. Here we tentatively assign this

https://doi.org/10.1021/acs.jpcc.6c01260
J. Phys. Chem. C 2026, 130, 6243−6259

Table 5. ^{17}O NMR Parameters for NBO and BO Sites in Various Single- and Mixed-Modifier Alkali and Alkaline-Earth Metaphosphate Glasses

composition	site	δ_{iso} (±0.5 ppm)	C_Q (±0.1 MHz)	η (±0.02)
$NaPO_3$	BO	120.0	7.5	0.37
	NBO	82.7	4.5	0.20
$LiPO_3$	BO	118.5	7.9	0.35
	NBO	81.3	4.7	0.22
$RbPO_3$	BO	125.2	7.6	0.36
	NBO	112.2	4.7	0.27
$Mg(PO_3)_2$	BO	114.6	8.1	0.34
	NBO	76.7	5.1	0.21
$Ca(PO_3)_2$	BO	118.7	7.4	0.43
	NBO	104.9	4.6	0.22
$Ba(PO_3)_2$	BO	121.9	7.4	0.39
	NBO	125.4	4.5	0.24
$NaMg_{0.5}(PO_3)_2$	BO	118.7	7.8	0.37
$NaCa_{0.5}(PO_3)_2$	BO	119.3	7.8	0.36
$NaBa_{0.5}(PO_3)_2$	BO	120.2	7.6	0.36
	NBO	132.0	4.5	0.26
$NaLi(PO_3)_2$	BO	119.3	7.9	0.36
$LiRb(PO_3)_2$	BO	121.8	7.5	0.35

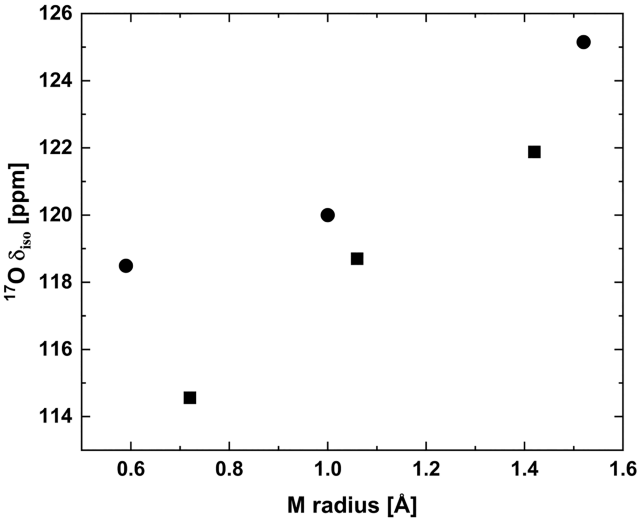

Figure 6. Variation of ^{17}O isotropic chemical shift of BO site in SM metaphosphate glasses with radius of alkali (circles) or alkaline-earth (squares) modifier cation. Error bars are within the size of symbols.

resonance to NBO sites in $[P_2O_7]^{4-}$ pyrophosphate units as such relatively high ^{17}O C_Q values were reported in the literature for the NBO sites in several alkali and alkaline-earth pyrophosphate crystals.[55,62]

As noted above, a 3QMAS NMR spectrum allows for obtaining distributions of the quadrupolar parameters C_Q and η as a function of the chemical shift for a specific structural site in a disordered material. These distributions of C_Q and η are obtained from simulation of slices of the BO resonance along the MAS dimension in the ^{17}O 3QMAS NMR spectra for all glasses except for the Ca and Ba-metaphosphates (Figure 8), where the BO signal is too weak and/or overlaps too strongly with the NBO signal for reliable analysis of the NMR line shapes. These distributions are generally similar in the sense that they all show relatively little change in C_Q within experimental error, while η decreases monotonically from ∼0.5 to ∼0.3 with decreasing δ_{iso}. Previous studies[66,68,69] indicated

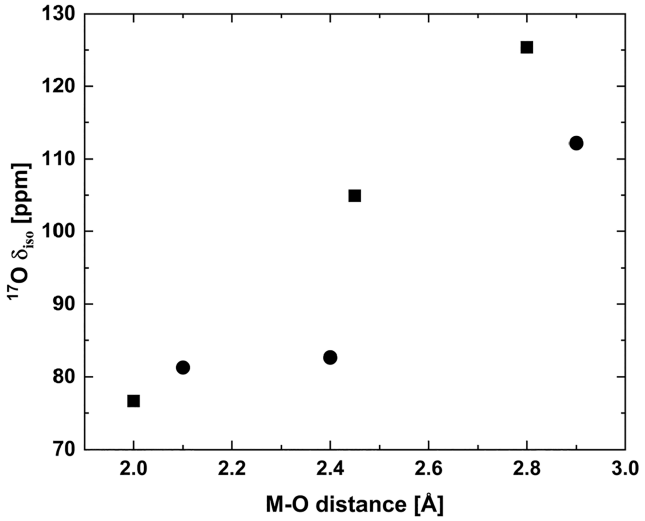

Figure 7. Variation of ^{17}O isotropic chemical shift of NBO site in SM metaphosphate glasses with alkali (circles) or alkaline-earth (squares) modifier cation−oxygen bond length. Error bars are within the size of symbols.

that these quadrupolar parameters for BO sites may be related to the associated bond angle θ (e.g., Si−O−Si or P−O−P angle). Therefore, the ^{17}O 3QMAS NMR spectra presents an opportunity to extract the P−O−P bond angle distribution (BAD) in these phosphate glasses from the corresponding distribution in η. Specifically, the ^{17}O NMR study of Na-phosphate glasses by Zeyer et al.[66] used the expression derived by Sternberg[75] between ^{17}O η and θ to calculate the average P−O−P angle in a $NaPO_3$ glass. This relationship can be written as[75]

$$\eta = \left[\frac{4}{1 - 3\cos\theta}\right] - 1 \quad (6)$$

However, eq 6 was derived on the basis of purely geometric arguments and did not take into account the electronic structure of the bonding environment. Therefore, instead of using eq 6, here we have built a correlation between ^{17}O η and θ based on experimental results as well as DFT-based calculations of η in a variety of crystalline alkali and alkaline-earth phosphate compounds (Table 3) as shown in Figure 9. A fit to this η vs θ data set yields

$$\eta = \left[\frac{3.9456}{1 - 3\cos\theta}\right] - 0.833 \quad (7)$$

We have used eq 7 to convert the distribution of η in Na, Li, Rb and Mg metaphosphate glasses as shown in Figure 8 to the corresponding P−O−P BAD (Figure 10). It is intriguing to note that the P−O−P BAD of $NaPO_3$ glass derived this way from ^{17}O 3QMAS NMR is strikingly similar to that reported by Marchin et al.[20] in a recent molecular dynamics study utilizing potentials that incorporated three-body interactions. This distribution shows a peak value of the P−O−P angle of ∼139° with a full-width-at-half-maximum (FWHM) of ∼10°. The peak of the P−O−P BAD shifts to a slightly higher value of ∼142° for the $LiPO_3$ and $Mg(PO_3)_2$ compositions. More importantly, the FWHM of this BAD increases significantly to ∼15° for the $Mg(PO_3)_2$ glass, while it was found to be somewhat narrower in the $RbPO_3$ glass. This limited data set suggests that the disorder in the P−O−P BAD increases with

https://doi.org/10.1021/acs.jpcc.6c01260
J. Phys. Chem. C 2026, 130, 6243−6259

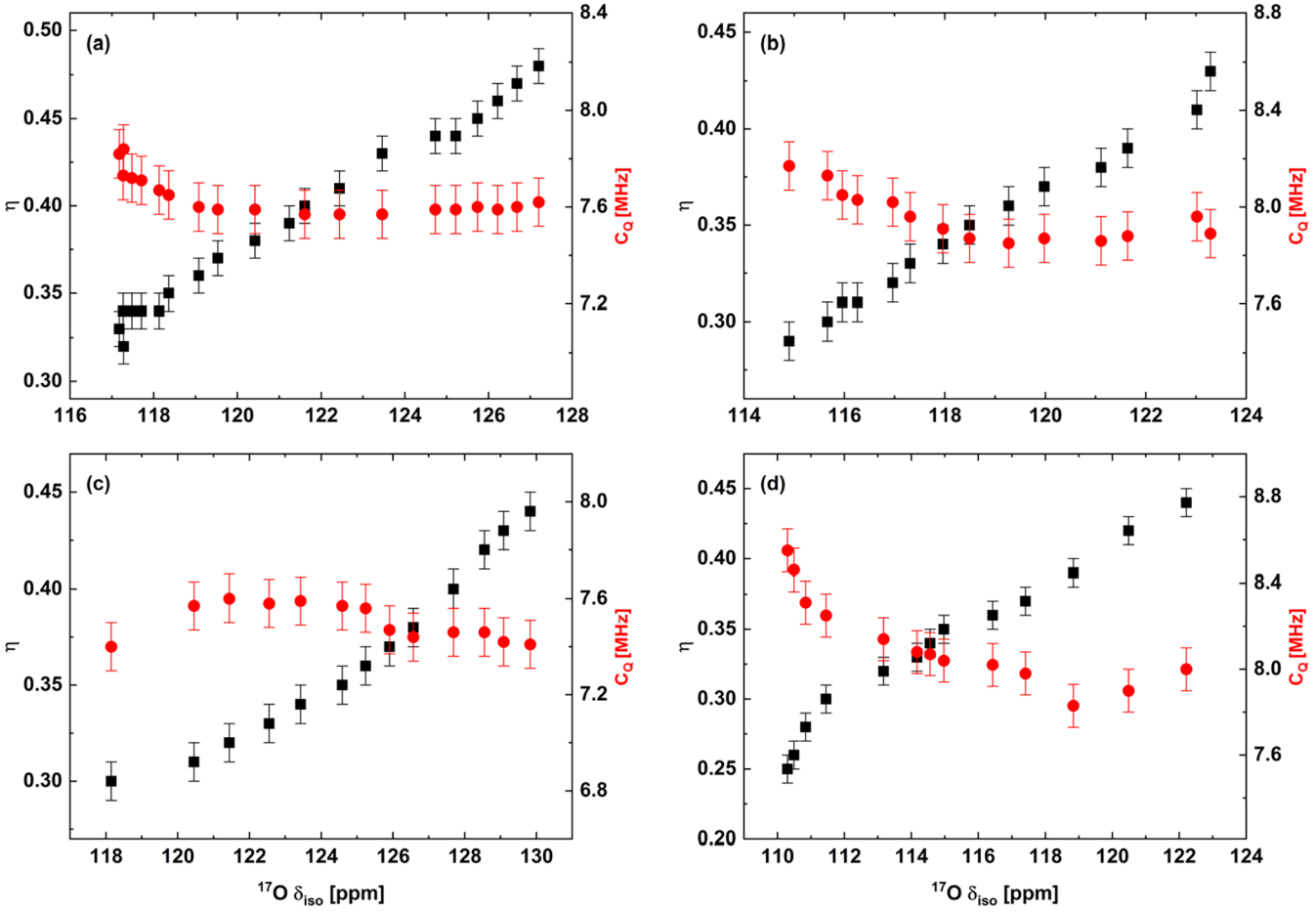

Figure 8. Variation of BO site ^{17}O quadrupolar parameters C_Q (circles) and η (squares) with ^{17}O isotropic chemical shift for (a) $NaPO_3$, (b) $LiPO_3$, (c) $RbPO_3$ and (d) $Mg(PO_3)_2$ glasses.

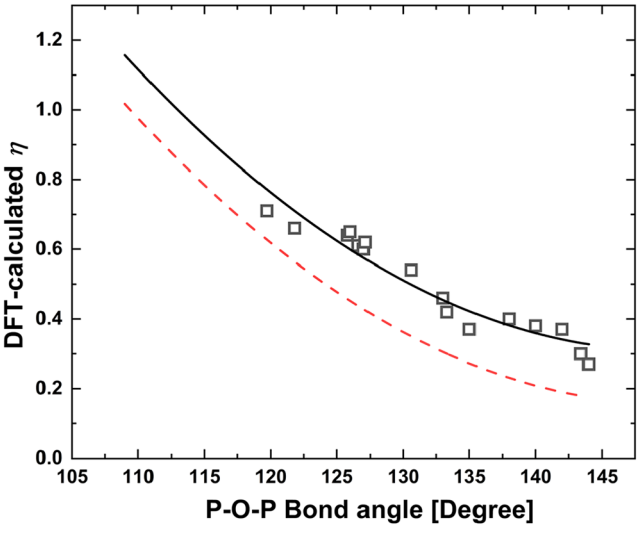

Figure 9. Variation of ^{17}O η calculated by DFT for BO sites in geometry optimized structures of select phosphate compounds (black squares) with corresponding P−O−P angle. Red dashed line and black solid line correspond to eqs 6 and 7, respectively, in the text.

increasing field strength of the M cation. This result can also explain the aforementioned trend reported in the literature of increasing ^{31}P FWHM of the Q^2 resonance in metaphosphate glasses with the M cation field strength.[63−65] The increased disorder in the P−O−P BAD implies increased folding or coiling of the Q^2 phosphate chains in these glasses. The phosphate chains in crystalline polyphosphates are indeed known to show increased contortion with increasing field strength of the M cation.[76] Such an effect is likely driven both by the valence of the M cation where the folding of the chain allows for an efficient charge compensation of the former, as well as by the fact that high−field-strength cations such as Mg^{2+} can strongly polarize the NBOs, thereby reducing repulsion between the PO_4 tetrahedra in the chains and favoring chain folding.[76]

3.2. Mixed-Modifier Metaphosphate Glasses and Spatial Distribution of M Cations

Previous ^{31}P NMR studies of mixed-alkali metaphosphate glasses in the literature have shown that the ^{31}P δ_{iso} decreases nearly linearly with progressive replacement of one alkali with another of higher field strength, while the Q-speciation remains unaffected.[64,65] A similar trend is also observed in the present study for the mixed-modifier (MM) metaphosphate glasses. Here we only show the ^{31}P MAS NMR spectra of select MM compositions that have not been previously reported in the literature to the best of our knowledge, namely the Na−Mg and Na−Ca metaphosphate glasses and compare them with the SM end members (Figure 11). These ^{31}P MAS NMR spectra also display an increase in the FWHM of the Q^2 resonance for the MM compositions compared to that for the corresponding end members.

https://doi.org/10.1021/acs.jpcc.6c01260
J. Phys. Chem. C 2026, 130, 6243−6259

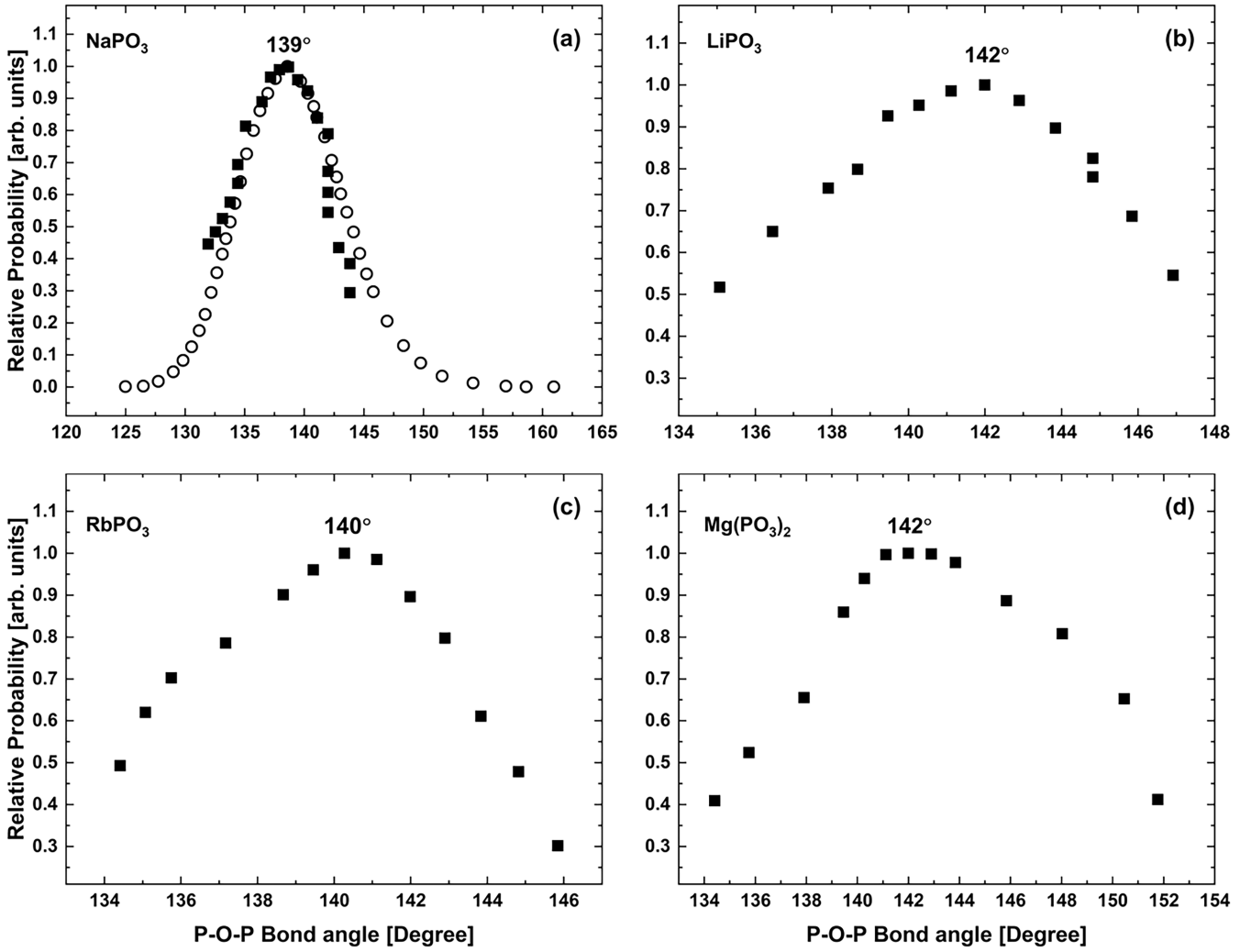

Figure 10. P−O−P BAD in (a) Na, (b) Li, (c) Rb and (d) Mg metaphosphate glasses (filled squares), calculated using eq 7 and experimental distribution of η for the BO site obtained from ^{17}O 3QMAS NMR spectra (see text for details). Open circles in top left panel denote P−O−P BAD in $NaPO_3$ glass, obtained in a recent study by molecular dynamics simulation.[20] All P−O−P angles are estimated to within ±1°.

Previous ^{17}O 3QMAS and Dynamic-Angle-Spinning (DAS) NMR spectroscopic studies of silicate and aluminosilicate glasses with MM cations have shown that an NBO site population analysis can provide unique information regarding the distribution of the M cations in the structure. Pioneering ^{17}O DAS NMR studies by Florian et al.[41] indicated random mixing between alkali cations such as Na and K in silicate glasses. On the other hand, ^{17}O 3QMAS NMR studies by Stebbins and co-workers indicated random mixing between alkaline-earths Ca and Ba,[42] while Na and Ca were found to be mixed more uniformly[43] in silicate glasses. In contrast, the high field-strength Mg in K−Mg silicate glasses was reported to show a clear preference for NBO, thereby pushing K cations to bond with BO while, Ca was reported to mix more randomly with Mg in (Ca, Mg)SiO_3 glasses.[44] A different behavior was reported for Ca in Ca−Mg aluminosilicates,[45] where NBOs were found to bond preferentially with Mg, thereby forcing Ca to have significant bonding interactions with BO atoms. Such preference was also reported to be dependent on the Al/Si ratio in these glasses.

Similar to the ^{17}O 3QMAS spectra of the SM alkali and alkaline-earth phosphate glasses, those for the MM metaphosphate glasses also show two distinct resonances, which can be readily assigned to NBO and BO sites (Figure 12). Following the methodology outlined in previous ^{17}O 3QMAS NMR studies by Stebbins and co-workers,[42−45] here we have analyzed the isotropic projections of the ^{17}O 3QMAS NMR spectra of the MM glasses and compared them to those of the SM end members in Figure 13. In the case of the Na−Li mixed-alkali series, the NBO peak for the MM composition has a FWHM similar to those for the end member compositions, while it is located at an intermediate position compared to the latter, implying intimate mixing of Na and Li in the structure of the MM glass. Before we attempt to interpret these results further, it may be insightful here to consider the possible NBO-M coordination environments in these glasses in terms of the bond valence (BV) model. According to the BV model the sum of bond valences at each atom is equal to the atomic valence of that atom.[77,78] In practice the equality in this valence sum rule is found to be valid to within 5−10%.[77,78] The bond valence s for P−O bonds in oxides is given by the expression[77]

$$s = \exp[-(R - R_0)/B] \quad (8)$$

where the empirical constants R_0 = 1.62 Å and B = 0.36, and R is the corresponding P−O bond length. For $NaPO_3$ glass the

https://doi.org/10.1021/acs.jpcc.6c01260
J. Phys. Chem. C 2026, 130, 6243−6259

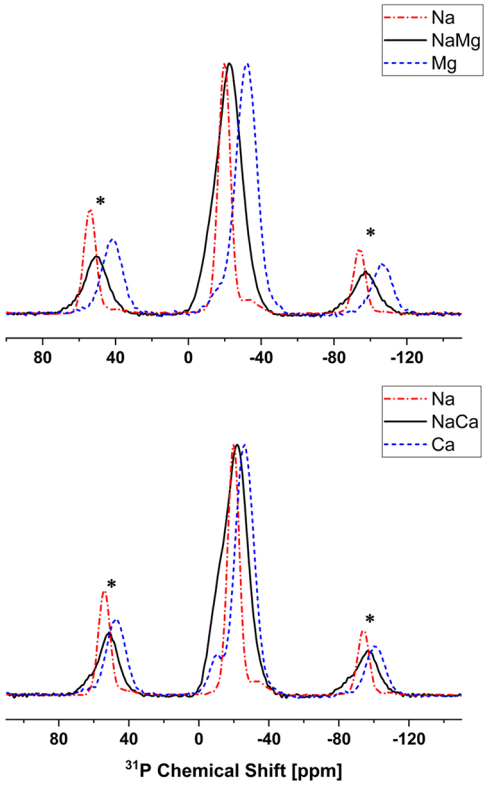

Figure 11. Comparison between ^{31}P MAS NMR spectra of mixed-modifier metaphosphate glasses (black solid line) and that of their respective end members (red dashed-dotted line and blue dashed line).

P-NBO = 1.48 Å[16,20] and consequently $s_{(P\text{-}NBO)}$ = 1.475. Since the absolute value of the atomic valence of oxygen is 2.0, the rest of the BV of 0.525 must come from M−O bonds. Experimentally, the Na−O bond distance in $NaPO_3$ glass has been observed to be 2.38 Å[16,20] and one can use the same empirical form of the BV expression as in eq 8 for the bond valence of the Na−O bond with R_0 = 1.661 Å and B = 0.44, which yields $s_{(Na\text{-}NBO)}$ = 0.195. Therefore, besides 1 P atom, the NBO is expected to be bonded to 2−3 Na atoms. Such environments are indeed present in the crystalline Na-trimetaphosphate $Na_3P_3O_9$.[55] On the other hand, the Li−O bond valence contribution can be calculated using eq 8, where R_0 = 1.292 Å and B = 0.48. The experimentally determined Li−O bond length R in the $LiPO_3$ glass is 2.0 Å[71] and thus, $s_{(Li\text{-}NBO)}$ = 0.23. This would indicate that the NBO in this glass is bonded to 2 to up to 3 Li atoms, and the former is observed in crystalline $LiPO_3$.[56] Therefore, for a random distribution of 2 (Na+Li) atoms around the NBOs, $O(Na)_2$, O(Na,Li), and $O(Li)_2$ sites would be present in 1:2:1 ratio. Similarly, for a total of 3 M atoms, the possible configurations $O(Na)_3$, $O(Na_2Li)$, $O(Li_2Na)$ and $O(Li)_3$ would be present in a 1:3:3:1 ratio for a random distribution. On the other hand, if Na and Li are uniformly distributed then there would be one NBO site of the type O(Na,Li). The other extreme structural scenario would be a fully clustered distribution with only $O(Na)_{2/3}$ and $O(Li)_{2/3}$ sites. In the case of the ^{17}O 3QMAS isotropic line shape of the Na−Li metaphosphate glasses (Figure 13e), the NBO peak for the MM composition overlaps too strongly with those for the end member compositions to distinguish between these mixing models, though the symmetric NBO peak of the (Na, Li)PO_3 glass with similar width and intermediate position compared to those of the end members strongly suggests a uniform or random mixing of Na and Li cations rather than a clustered distribution.

In the case of the Li, Rb metaphosphate glasses, the BV contribution of the Rb−O bond can be calculated from the relation[77]

$$s = (R/R_0)^{-N} \tag{9}$$

where the empirical constants R_0 = 2.22 Å and N = 7.0, which yields $s_{(Rb\text{-}NBO)}$ = 0.15 for typical experimental Rb−O bond length of 2.9 Å in $RbPO_3$ glass.[71] Consequently, the NBO in the $RbPO_3$ glass is likely bonded to 3 Rb atoms to satisfy the atomic valence of the oxygen, as is the case for crystalline $RbPO_3$.[72] Therefore, for a random distribution, the four possible NBO environments in the (Li,Rb)PO_3 glass $O(Li)_3$, $O(Li_2Rb)$, $O(LiRb_2)$, and $O(Rb)_3$ would be present in a 1:3:3:1 ratio. The ^{17}O 3QMAS isotropic spectrum of the (Li,Rb)PO_3 glass (Figure 13c) shows a main peak that is broader than the NBO peaks for the end member compositions and its center of gravity is located between those of the end member glasses, though it is shifted more toward the peak for the $LiPO_3$ end member. This result qualitatively suggests significant mixing between Li and Rb ions in the glass structure. Additionally, the NBO resonance in this spectrum displays a clear shoulder located at 112 ppm that is similar to the location of the NBO peak in the $RbPO_3$ glass (Figure 13c) corresponding to the $O(Rb)_3$ sites. Simulation of the ^{17}O isotropic spectral line shape for the NBO resonance of the (Li, Rb)PO_3 glass with Gaussian line shapes and peak area integration shows that this shoulder constitutes about ∼16% of the NBO signal in the (Li, Rb)PO_3 glass. It may be noted here that such simulations yield quantitative results as the NBOs in all glasses are characterized by a narrow range of C_Q, which implies uniform 3QMAS excitation efficiency. Therefore, approximately 16% of the NBO in this MM glass is in the form of $O(Rb)_3$ sites, while a perfectly random distribution of Li and Rb would predict the relative fraction of the $O(Rb)_3$ sites to be 12.5%. These observations, when taken together, indicate that the Li and Rb distribution around the NBO atoms in the (Li, Rb)PO_3 glass is close to random.

Finally, in the case of alkali−alkaline-earth MM metaphosphate glasses, the BV contribution from the Mg−O, Ca−O and Ba−O bonds can be calculated using either eq 8 or eq 9, using the empirical parameters listed in ref 77 and the typical bond lengths of 2.0, 2.4, and 2.8 Å, respectively, as reported in the literature for these metaphosphate glasses.[16−18] The resulting BV values are $s_{(Mg\text{-}NBO)}$ = 0.41, $s_{(Ca\text{-}NBO)}$ = 0.29, and $s_{(Ba\text{-}NBO)}$ = 0.25. Therefore, considering $s_{(P\text{-}NBO)}$ = 1.475, each NBO in the end member alkaline-earth metaphosphate compositions can be bonded to 1 Mg, 2 Ca or 2 Ba atoms. The ^{17}O isotropic spectrum of the Na−Mg metaphosphate glass (Figure 13b) shows an NBO peak that is located nearly at the same position as the NBO peak for the $NaPO_3$ glass and is only slightly broader than that of the latter. These NBO peaks significantly overlap with the NBO peak of the $Mg(PO_3)_2$ glass, although the latter peak is significantly broader. Therefore, considering that Na and Mg are present in 2:1 ratio in the Na,Mg metaphosphate glass we argue that the NBO peak in the MM glass likely corresponds to two types of NBO sites, one with NBO bonded to ∼3 Na atoms as in the $NaPO_3$ glass and the other with NBO bonded to 1 Mg and 1 Na atom to satisfy the required BV sum of 2.0 to within ±10% as well as to satisfy a spatially uniform charge distribution from the M cations

https://doi.org/10.1021/acs.jpcc.6c01260
J. Phys. Chem. C 2026, 130, 6243−6259

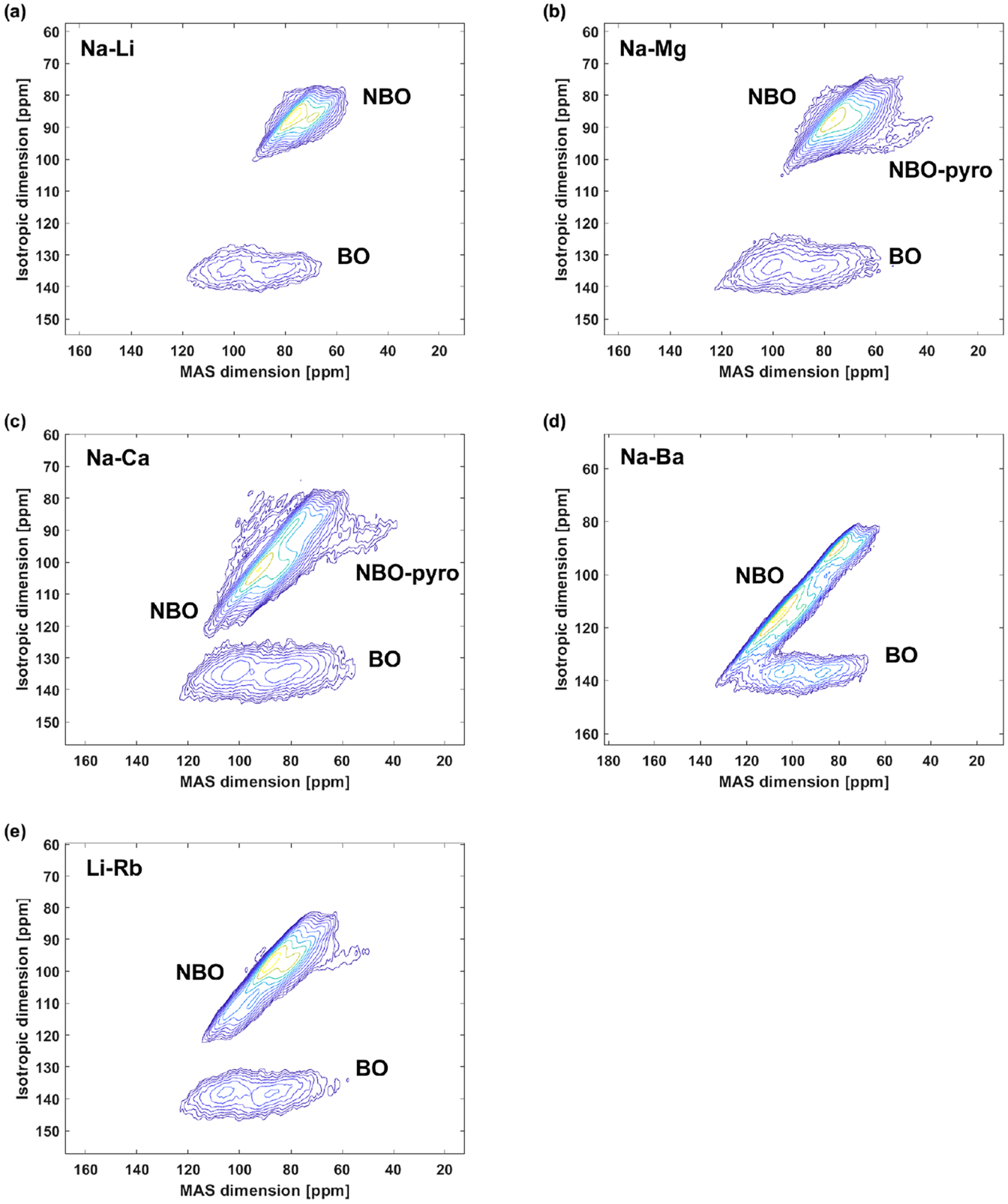

Figure 12. Contour plots of ^{17}O 3QMAS NMR spectra of mixed-modifier (a) Na−Li, (b) Na−Mg, (c) Na−Ca, (d) Na−Ba and (e) Li−Rb MM metaphosphate glasses. NBO and BO sites corresponding to the Q^2 species and Q^1-NBO sites (NBO-pyro) are denoted alongside the contours.

around the NBOs. This scenario therefore suggests a relatively ordered distribution of Na and Mg atoms in this glass.

Finally, the ^{17}O isotropic spectra of the Na−Ba and Na−Ca metaphosphate glass (Figures 13d and 13a) shows a rather broad NBO peak with constituent resonances located at positions intermediate to those that are characteristic of the end members, indicating significant mixing between these two M cations in the glass structure. Both spectra contain a relatively well-resolved resonance located nearly at the same position as the NBO peak for the $NaPO_3$ glass. Simulation of

https://doi.org/10.1021/acs.jpcc.6c01260
J. Phys. Chem. C 2026, 130, 6243−6259

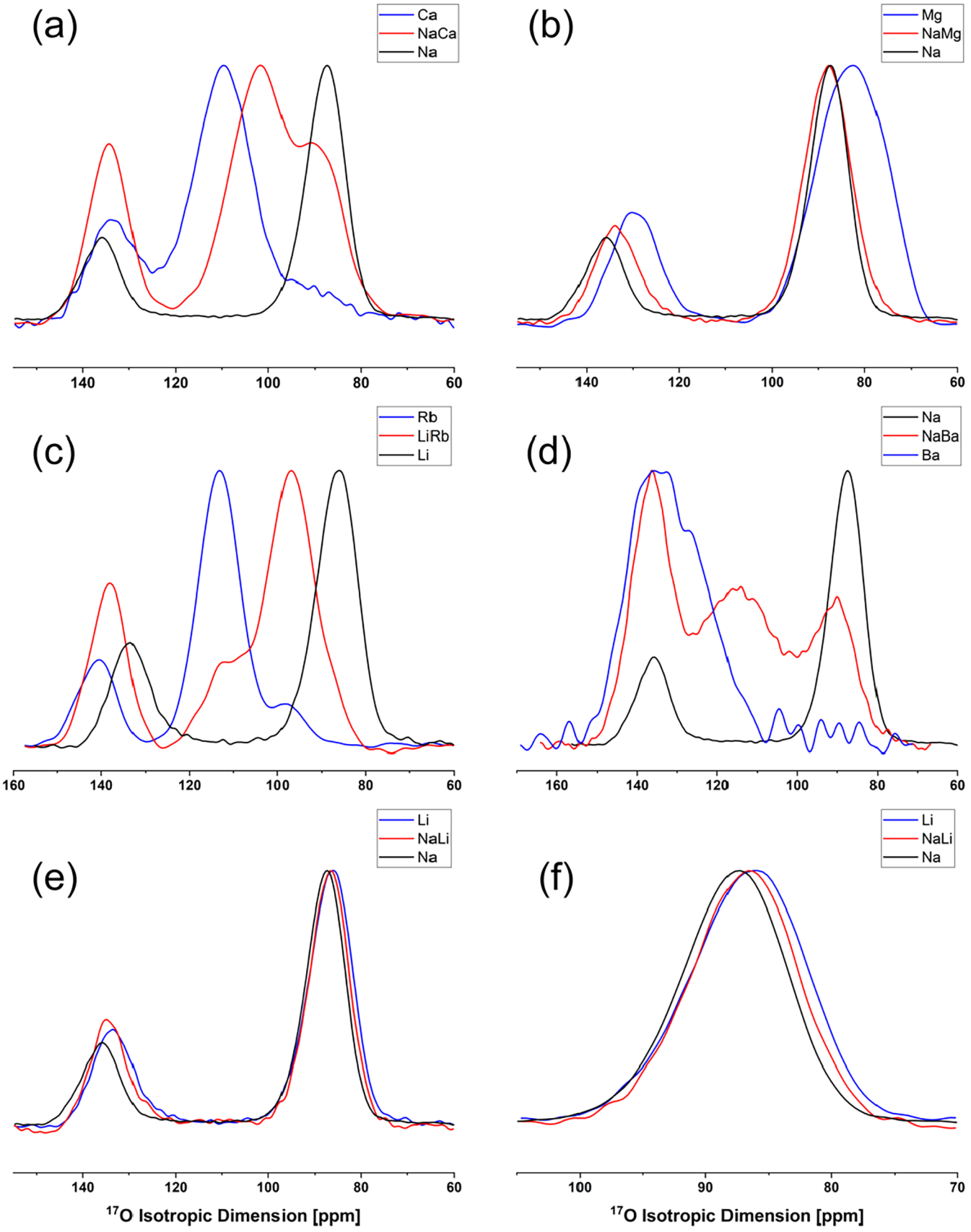

Figure 13. ^{17}O 3QMAS isotropic projection spectra of MM metaphosphates (red lines) and of their SM metaphosphate end members (black and blue lines) for (a) Na−Ca, (b) Na−Mg, (c) Li−Rb, (d) Na−Ba, and (e) Na−Li systems. Expanded view of the NBO resonances in the spectra in (e) is shown in (f).

https://doi.org/10.1021/acs.jpcc.6c01260
J. Phys. Chem. C 2026, 130, 6243−6259

these isotropic spectra with Gaussian line shapes yield a relative fraction for this NBO peak of ~31% for the Na−Ba composition and ~35% for the Na−Ca composition. These values indicate that nearly one-third of the NBOs are in ONa_3 configuration and not bonded to Ca or Ba. Again considering that Na/Ca or Na/Ba cation ratio in these MM glasses is 2:1, this relative fraction of NBOs in ONa_3 configuration would indeed be expected for a uniform mixing between Na and Ca or Ba around NBOs in O(Na, Ca) or O(Na, Ba) configurations with the rest of the Na being in ONa_3 configuration.

It is therefore important to note that bivalent alkaline-earth cations behave differently from monovalent alkalis such as Rb and Li in their mixing behavior with Na, with the former being more uniform with preference for pairing between dissimilar cations while the latter being more random. This general observation in phosphates is broadly consistent with that reported for silicates and it likely results from the preference of the structure to maximize a uniform spatial distribution of charges associated with the modifier cations. Such difference in the mixing behavior between two alkalis vs an alkali and an alkaline-earth cations can have important consequences for ionic transport in these glasses as well as for the configurational entropy of the parent supercooled liquids. For example, for a random distribution of dissimilar alkali cations, the hopping path of one cation can be most efficiently blocked by the presence of the other due to the mismatch in their site geometry and this blocking effect will be maximized for subequal concentration of the two cations, leading to a minimum in ionic conductivity. This nonlinear composition dependence of ionic conductivity is well-known in the literature as the mixed-alkali effect.[79−84] On the other hand, for a uniform distribution of two dissimilar cations, the ionic mobility will be expected to decrease monotonically with composition as the mobile alkali cation is progressively replaced by a relatively immobile alkaline-earth cation. Such a monotonic behavior of ionic conductivity has indeed been reported in the literature for mixed alkali−alkaline-earth phosphate glasses.[85−87] The configurational entropy of mixing of the M cations has been linked in the literature to the mixed-alkali effect on the glass transition temperature T_g and isothermal viscosity. Clearly, this entropic contribution will be maximized for a random distribution of dissimilar M cations as observed here for the mixed-alkali metaphosphates and will decrease with increased ordering in the distribution and thus will likely be very small for mixed alkali−alkaline earth metaphosphates. This expectation is consistent with the experimental observation made in previous studies that a strong mixed-cation effect on T_g and viscosity is only observed in the case of mixed-alkali systems, while mixed alkali−alkaline-earth systems show a monotonic variation of these dynamic properties with the makeup of the M cations.[85,88]

As noted above, the ^{17}O δ_{iso} for the BO sites show systematic decrease with increasing field strength of the M cations in SM metaphosphates and the BO ^{17}O δ_{iso} for any MM metaphosphate glass is located at values that are intermediate between those of the corresponding SM end members (Table 5). It may be noted here that the dependence of BO ^{17}O δ_{iso} on the nature of the modifier cation is rather small compared to the large range of δ_{iso} displayed by the NBO sites, consistent with the expected relatively weak interaction between the modifiers and BO in phosphate glasses. However, these small but systematic changes in BO ^{17}O δ_{iso} may originate from a systematic change in the P−O−P angle with changing field strength of the M cations. In order to test this hypothesis, the P−O−P BAD for the Li−Rb and Na−Mg MM metaphosphates are calculated (Figure 14) following the procedure outlined above for the SM metaphosphate glasses. The resulting average P−O−P angle is indeed observed to increase upon replacement of Rb with Li and of Na with Mg as the corresponding BO ^{17}O δ_{iso} decreases (Figure 15), thus providing support to the above hypothesis.

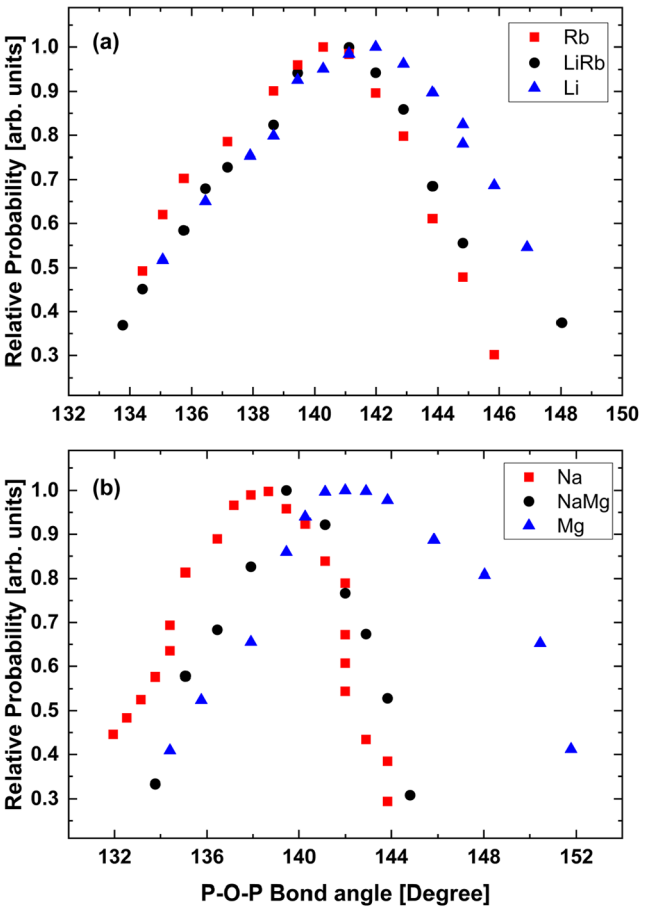

Figure 14. P−O−P BAD in (a) Li−Rb and (b) Na−Mg MM metaphosphate glasses (circles), calculated using eq 7 and experimental distribution of η for the BO site obtained from ^{17}O 3QMAS NMR spectra (see text for details). BAD of corresponding single-modifier end members are shown (squares and triangles) for comparison. All P−O−P angles are estimated to within ±1°.

4. CONCLUSIONS

The tetrahedral chain conformation, modifier-oxygen interaction and spatial distribution of dissimilar modifier cations are studied in SM and MM metaphosphate glasses using high-resolution ^{31}P and ^{17}O NMR spectroscopy. While ^{31}P NMR spectra provide information on Q^n tetrahedral speciation, ^{17}O 3QMAS NMR spectra of these glasses are shown to provide site-specific insight into both bridging (P−O−P) and non-bridging (P−O−M) oxygen environments. The large contrast in quadrupolar coupling constants between BO and NBO sites directly reflects the higher covalency of P−O−P linkages relative to modifier-coordinated NBO environments, while systematic trends in ^{17}O isotropic chemical shifts reveal a strong dependence of NBO electronic structure on M−O bond

https://doi.org/10.1021/acs.jpcc.6c01260
J. Phys. Chem. C 2026, 130, 6243−6259

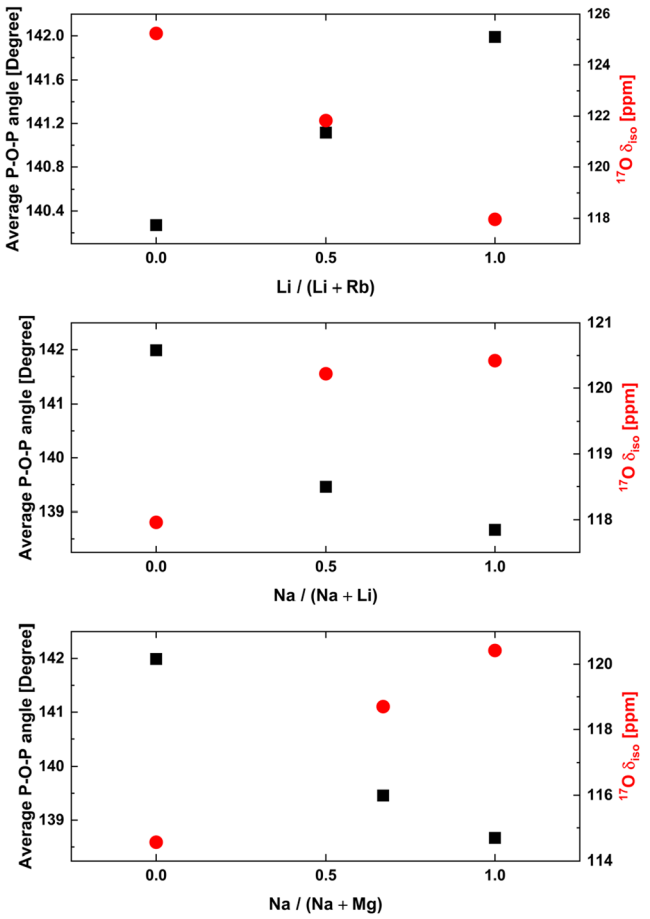

Figure 15. Compositional variation of average P−O−P angle and ^{17}O isotropic chemical shift for BO sites in Li−Rb (top), Na−Li (middle) and Na−Mg (bottom) metaphosphate glasses.

distance and modifier field strength. A correlation between the ^{17}O quadrupolar asymmetry parameter η and the P−O−P bond angle is established using DFT calculations on crystalline phosphates, enabling direct extraction of the P−O−P BADs of these glasses from the ^{17}O 3QMAS spectra. The resulting BADs show increasing average P−O−P angle and increasing disorder with increasing modifier field strength, consistent with enhanced contortion of phosphate chains. These results also provide an atomistic explanation for previously reported trends in ^{31}P line widths in SM vs MM metaphosphate systems.

In MM metaphosphate glasses, analysis of ^{17}O 3QMAS isotropic projection line shapes combined with bond-valence considerations reveals predominantly uniform mixing between monovalent alkali and bivalent alkaline-earth cations, while a nearly random mixing behavior is displayed by dissimilar monovalent alkali cations. Such contrasting behavior is hypothesized to be driven by the tendency for maintaining spatial uniformity in the charge distribution and is argued to be a key controlling factor for the mixed-modifier effect on the transport properties in glasses and corresponding supercooled liquids.

AUTHOR INFORMATION

Corresponding Author

Sabyasachi Sen − *Department of Materials Science and Engineering, University of California at Davis, Davis, California 95616, United States;* orcid.org/0000-0002-4504-3632; Email: sbsen@ucdavis.edu

Authors

Shih-Yi Chuang − *Department of Materials Science and Engineering, University of California at Davis, Davis, California 95616, United States*

Ivan Hung − *National High Magnetic Field Laboratory, Tallahassee, Florida 32310, United States;* orcid.org/0000-0001-8916-739X

Zhehong Gan − *National High Magnetic Field Laboratory, Tallahassee, Florida 32310, United States;* orcid.org/0000-0002-9855-5113

Complete contact information is available at: https://pubs.acs.org/10.1021/acs.jpcc.6c01260

Notes

The authors declare no competing financial interest.

ACKNOWLEDGMENTS

This work was supported by an NSF grant (DMR 2409281) to S.S. The National High Magnetic Field Laboratory is supported by the National Science Foundation through NSF/DMR-2128556 and the State of Florida.

REFERENCES

(1) Wilder, J. A. Glasses and Glass Ceramics for Sealing to Aluminum Alloys. *J. Non-Cryst. Solids* **1980**, *38*−*39*, 879−884.

(2) Campbell, J. H.; Suratwala, T. I. Nd-Doped Phosphate Glasses for High-Energy/High-Peak-Power Lasers. *J. Non-Cryst. Solids* **2000**, *263*−*264*, 318−341.

(3) Boetti, N.; Pugliese, D.; Ceci-Ginistrelli, E.; Lousteau, J.; Janner, D.; Milanese, D. Highly Doped Phosphate Glass Fibers for Compact Lasers and Amplifiers: A Review. *Appl. Sci.* **2017**, *7* (12), No. 1295.

(4) Knowles, J. C. Phosphate Based Glasses for Biomedical Applications. *J. Mater. Chem.* **2003**, *13* (10), 2395−2401.

(5) Sharmin, N.; Rudd, C. D. Structure, Thermal Properties, Dissolution Behaviour and Biomedical Applications of Phosphate Glasses and Fibres: A Review. *J. Mater. Sci.* **2017**, *52* (15), 8733−8760.

(6) Ehrt, D. Review: Phosphate and Fluoride Phosphate Optical Glasses—Properties, Structure and Applications. *Phys. Chem. Glasses: Eur. J. Glass Sci. Technol., Part B* **2015**, *56* (6), 217−234.

(7) Liu, J.; Wang, F.; Liao, Q.; Zhu, H.; Liu, D.; Zhu, Y. Synthesis and Characterization of Phosphate-Based Glass-Ceramics for Nuclear Waste Immobilization: Structure, Thermal Behavior, and Chemical Stability. *J. Nucl. Mater.* **2019**, *513*, 251−259.

(8) Oelkers, E. H.; Montel, J.-M. Phosphates and Nuclear Waste Storage. *Elements* **2008**, *4* (2), 113−116.

(9) Fu, J. Fast Li^+ Ion Conduction in Li_2O-(Al_2O_3 Ga_2O_3)-TiO_2-P_2O_5 Glass-Ceramics. *J. Mater. Sci.* **1998**, *33*, 1549−1553.

(10) Brow, R. K. Review: The Structure of Simple Phosphate Glasses. *J. Non-Cryst. Solids* **2000**, *263*−*264*, 1−28.

(11) Kirkpatrick, R. J.; Brow, R. K. Nuclear Magnetic Resonance Investigation of the Structures of Phosphate and Phosphate-Containing Glasses: A Review. *Solid State Nucl. Magn. Reson.* **1995**, *5* (1), 9−21.

(12) Fayon, F.; Massiot, D.; Suzuya, K.; Price, D. L. ^{31}P NMR Study of Magnesium Phosphate Glasses. *J. Non-Cryst. Solids* **2001**, *283* (1−3), 88−94.

(13) Xia, Y.; Chen, H.; Hung, I.; Gan, Z.; Sen, S. Structure and Fragility of Zn-Phosphate Glasses: Results from Multinuclear NMR Spectroscopy and Calorimetry. *J. Non-Cryst. Solids* **2022**, *580*, No. 121395.

(14) Jäger, C.; Hartmann, P.; Witter, R.; Braun, M. New 2D NMR Experiments for Determining the Structure of Phosphate Glasses: A Review. *J. Non-Cryst. Solids* **2000**, *263*−*264*, 61−72.
(15) Feike, M.; Jager, C.; Spiess, H. W. Connectivities of Coordination Polyhedra in Phosphate Glasses from ^{31}P Double-Quantum NMR Spectroscopy. *J. Non-Cryst. Solids* **1998**, *223*, 200−206.
(16) Hoppe, U.; Stachel, D.; Beyer, D. The Oxygen Coordination of Metal Ions in Phosphate and Silicate Glasses Studied by a Combination of X-Ray and Neutron Diffraction. *Phys. Scr.* **1995**, *T57*, 122−126.
(17) Hoppe, U.; Walter, G.; Kranold, R.; Stachel, D. Structural Specifics of Phosphate Glasses Probed by Diffraction Methods: A Review. *J. Non-Cryst. Solids* **2000**, *263*, 29−47.
(18) Hoppe, U.; Walter, G.; Stachel, D.; Barz, A.; Hannon, A. C. Neutron and X-Ray Diffraction Study on the Structure of Ultraphosphate Glasses. *Z. Naturforsch. A* **1997**, *52* (3), 259−269.
(19) Kalahe, J.; Mahadevan, T. S.; Lu, X.; Vienna, J. D.; Riley, B. J.; Du, J. Insights on the Structure and Properties of Sodium Iron Phosphate Glasses from Molecular Dynamics Simulations. *J. Nucl. Mater.* **2024**, *594*, No. 155004.
(20) Marchin, N.; Urata, S.; Du, J. Effect of Three-Body Interaction on Structural Features of Phosphate Glasses from Molecular Dynamics Simulations. *J. Chem. Phys.* **2024**, *161* (15), No. 154507.
(21) Tsuchida, J.; Schneider, J.; Deshpande, R. R.; Eckert, H. Cation Distribution and Local Order in Mixed Sodium Metaphosphate Glasses. *J. Phys. Chem. C* **2012**, *116* (46), 24449−24461.
(22) Zwanziger, J. W.; McLaughlin, J. C.; Tagg, S. L. Sodium Distribution in Sodium Tellurite Glasses Probed with Spin-Echo NMR. *Phys. Rev. B* **1997**, *56* (9), No. 5243.
(23) Voigt, U.; Lammert, H.; Eckert, H.; Heuer, A. Cation Clustering in Lithium Silicate Glasses: Quantitative Description by Solid-State NMR and Molecular Dynamics Simulations. *Phys. Rev. B* **2005**, *72* (6), No. 064207.
(24) Gee, B.; Eckert, H. Cation Distribution in Mixed-Alkali Silicate Glasses. NMR Studies by ^{23}Na−{^{7}Li} and ^{23}Na−{^{6}Li} Spin Echo Double Resonance. *J. Phys. Chem. A* **1996**, *100* (9), 3705−3712.
(25) Eckert, H. Spying with Spins on Messy Materials: 60 Years of Glass Structure Elucidation by NMR Spectroscopy. *Int. J. Appl. Glass Sci.* **2018**, *9* (2), 167−187.
(26) Eckert, H. Short and Medium Range Order in Ion-Conducting Glasses Studied by Modern Solid State NMR Techniques. *Z. Phys. Chem.* **2010**, *224* (10−12), 1591−1653.
(27) Strojek, W.; Eckert, H. Medium-Range Order in Sodium Phosphate Glasses: A Quantitative Rotational Echo Double Resonance Solid State NMR Study. *Phys. Chem. Chem. Phys.* **2006**, *8* (19), 2276−2285.
(28) Corbridge, D. E. C. The Crystal Structure of Sodium Triphosphate, $Na_5P_3O_{10}$, Phase I. *Acta Crystallogr.* **1960**, *13* (3), 263−269.
(29) Davies, D. R.; Corbridge, D. E. C. The Crystal Structure of Sodium Triphosphate, $Na_5P_3O_{10}$, Phase II. *Acta Crystallogr.* **1958**, *11* (5), 315−319.
(30) Leung, K. Y.; Calvo, C. The Structure of $Na_4P_2O_7$ at 22 °C. *Can. J. Chem.* **1972**, *50* (16), 2519−2526.
(31) Ondik, H. M. The Structure of Anhydrous Sodium Trimetaphosphate $Na_3P_3O_9$, and the Monohydrate, $Na_3P_3O_9.H_2O$. *Acta Crystallogr.* **1965**, *18* (2), 226−232.
(32) Averbuch-Pouchot, M. T. Structural Investigation of a New Series of Long-Chain Polyphosphates. Crystal Structure of AgK$(PO_3)_2$ and Crystal Data for Ag$M(PO_3)_2$ with M = K, Rb, Cs, and Ti. *J. Solid State Chem.* **1993**, *102* (1), 93−99.
(33) Jost, V. K. H. Die Struktur des Kaliumpolyphosphats $(KPO_3)_x$. *Acta Crystallogr.* **1963**, *16* (7), 623−626.
(34) Zachariasen, W. H. The Atomic Arrangement in Glass. *J. Am. Chem. Soc.* **1932**, *54* (10), 3841−3851.
(35) Greaves, G. N. EXAFS and the Structure of Glass. *J. Non-Cryst. Solids* **1985**, *71* (1−3), 203−217.
(36) Greaves, G. N.; Sen, S. Inorganic Glasses, Glass-Forming Liquids and Amorphizing Solids. *Adv. Phys.* **2007**, *56* (1), 1−166.
(37) Sidebottom, D. L.; Tran, T. D.; Schnell, S. E. Building up a Weaker Network: The Effect of Intermediate Range Glass Structure on Liquid Fragility. *J. Non-Cryst. Solids* **2014**, *402*, 16−20.
(38) Sidebottom, D. L. Fragility of Network-Forming Glasses: A Universal Dependence on the Topological Connectivity. *Phys. Rev. E* **2015**, *92* (6), No. 062804.
(39) Xia, Y.; Zhu, W.; Lockhart, M.; Aitken, B.; Sen, S. Fragility and Rheological Behavior of Metaphosphate Liquids: Insights into Their Chain vs. Network Characters. *J. Non-Cryst. Solids* **2019**, *514*, 77−82.
(40) Xia, Y.; Chen, H.; Aitken, B.; Sen, S. Rheological Characterization of Complex Dynamics in Na−Zn Metaphosphate Glass-Forming Liquids. *J. Chem. Phys.* **2021**, *155* (5), No. 054503.
(41) Florian, P.; Vermillion, K. E.; Grandinetti, P. J.; Farnan, I.; Stebbins, J. F. Cation Distribution in Mixed Alkali Disilicate Glasses. *J. Am. Chem. Soc.* **1996**, *118* (14), 3493−3497.
(42) Stebbins, J. F.; Oglesby, J. V.; Xu, Z. Disorder among Network-Modifier Cations in Silicate Glasses; New Constraints from Triple-Quantum ^{17}O NMR. *Am. Mineral.* **1997**, *82* (11−12), 1116−1124.
(43) Lee, S. K.; Stebbins, J. F. Nature of Cation Mixing and Ordering in Na-Ca Silicate Glasses and Melts. *J. Phys. Chem. B* **2003**, *107* (14), 3141−3148.
(44) Allwardt, J. R.; Stebbins, J. F. Ca-Mg and K-Mg Mixing around Non-Bridging O Atoms in Silicate Glasses: An Investigation Using ^{17}O MAS and 3QMAS NMR. *Am. Mineral.* **2004**, *89* (5−6), 777−784.
(45) Kelsey, K. E.; Allwardt, J. R.; Stebbins, J. F. Ca−Mg Mixing in Aluminosilicate Glasses: An Investigation Using ^{17}O MAS and 3QMAS and ^{27}Al MAS NMR. *J. Non-Cryst. Solids* **2008**, *354* (40−41), 4644−4653.
(46) Massiot, D.; Fayon, F.; Capron, M.; King, I.; Le Calvé, S.; Alonso, B.; Durand, J.; Bujoli, B.; Gan, Z.; Hoatson, G. Modelling One- and Two-dimensional Solid-state NMR Spectra. *Magn. Reson. Chem.* **2002**, *40* (1), 70−76.
(47) Haeberlen, U. *High Resolution NMR in Solids Selective Averaging: Supplement 1 Advances in Magnetic Resonance*; Academic Press, 1976.
(48) Brown, S. P.; Wimperis, S. Two-Dimensional Multiple-Quantum MAS NMR of Quadrupolar Nuclei. Acquisition of the Whole Echo. *J. Magn. Reson.* **1997**, *124* (1), 279−285.
(49) Brown, S. P.; Heyes, S. J.; Wimperis, S. Two-Dimensional MAS Multiple-Quantum NMR of Quadrupolar Nuclei. Removal of Inhomogeneous Second-Order Broadening. *J. Magn. Reson., Ser. A* **1996**, *119* (2), 280−284.
(50) Gan, Z.; Kwak, H.-T. Enhancing MQMAS Sensitivity Using Signals from Multiple Coherence Transfer Pathways. *J. Magn. Reson.* **2004**, *168* (2), 346−351.
(51) Grandinetti, P. J.; Baltisberger, J. H.; Llor, A.; Lee, Y. K.; Werner, U.; Eastman, M. A.; Pines, A. Pure-Absorption-Mode Lineshapes and Sensitivity in Two-Dimensional Dynamic-Angle Spinning NMR. *J. Magn. Reson., Ser. A* **1993**, *103* (1), 72−81.
(52) Pickard, C. J.; Mauri, F. All-Electron Magnetic Response with Pseudopotentials: NMR Chemical Shifts. *Phys. Rev. B* **2001**, *63* (24), No. 245101.
(53) Yates, J. R.; Pickard, C. J.; Mauri, F. Calculation of NMR Chemical Shifts for Extended Systems Using Ultrasoft Pseudopotentials. *Phys. Rev. B* **2007**, *76* (2), No. 024401.
(54) Bonhomme, C.; Gervais, C.; Babonneau, F.; Coelho, C.; Pourpoint, F.; Azaïs, T.; Ashbrook, S. E.; Griffin, J. M.; Yates, J. R.; Mauri, F.; Pickard, C. J. First-Principles Calculation of NMR Parameters Using the Gauge Including Projector Augmented Wave Method: A Chemist's Point of View. *Chem. Rev.* **2012**, *112* (11), 5733−5779.
(55) Vasconcelos, F.; Cristol, S.; Paul, J.-F.; Tricot, G.; Amoureux, J.-P.; Montagne, L.; Mauri, F.; Delevoye, L. ^{17}O Solid-State NMR and First-Principles Calculations of Sodium Trimetaphosphate $(Na_3P_3O_9)$, Tripolyphosphate $(Na_5P_3O_{10})$, and Pyrophosphate $(Na_4P_2O_7)$. *Inorg. Chem.* **2008**, *47* (16), 7327−7337.

https://doi.org/10.1021/acs.jpcc.6c01260
J. Phys. Chem. C 2026, 130, 6243−6259

(56) Murashova, E. V.; Chudinova, N. N. Synthesis and Crystal Structures of Lithium Polyphosphates, $LiPO_3$, $Li_4H(PO_3)_5$, and $LiMn(PO_3)_3$. *Crystallogr. Rep.* **2001**, *46* (6), 942−947.
(57) Grenier, J.-C.; Martin, C.; Durif-Varambon, A.; Tranqui, D.; Guitel, J.-C. Une nouvelle forme du métaphosphate de baryum $Ba(PO_3)_2$. *Bull. Soc. Fr. Mineral. Cristallogr.* **1967**, *90* (1), 24−31.
(58) Heyward, C.; Mann, M.; Kolis, J. Hydrothermally Synthesized α-$Ba_2P_2O_7$. *Acta Crystallogr., Sect. E: Struct. Rep. Online* **2010**, *66* (12), i84.
(59) Calvo, C. The Crystal Structure of α-$Mg_2P_2O_7$. *Acta Crystallogr.* **1967**, *23*, 289−295.
(60) Averbuch-Pouchot, M.-T. $CaNa_2P_4O_{12}$, a New Compound in the $Ca(PO_3)_2$-$NaPO_3$ System. *Eur. J. Solid State Inorg. Chem.* **1996**, *33*, 15−18.
(61) Martin, C.; Mitschler, A. Structure Cristalline Du Triméta-phosphate de Baryum−Sodium: $BaNaP_3O_9$. *Acta Crystallogr., Sect. B: Struct. Sci.* **1972**, *28* (8), 2348−2352.
(62) Prochnow, D.; Grimmer, A.-R.; Freude, D. Solid-State NMR Studies of ^{17}O-Enriched Pyrophosphates. *Solid State Nucl. Magn. Reson.* **2006**, *30* (2), 69−74.
(63) Brow, R. K.; Phifer, C. C.; Turner, G. L.; Kirkpatrick, R. J. Cation Effects on ^{31}P MAS NMR Chemical Shifts of Metaphosphate Glasses. *J. Am. Ceram. Soc.* **1991**, *74* (6), 1287−1290.
(64) Sato, R. K.; Kirkpatrick, R. J.; Brow, R. K. Structure of Li,Na Metaphosphate Glasses by ^{31}P and ^{23}Na MAS-NMR Correlated with the Mixed Alkali Effect. *J. Non-Cryst. Solids* **1992**, *143*, 257−264.
(65) Dos Santos, I. M. N.; De Melo Marques, F. A.; Munõz, A. M. N.; Rodrigues, A. C. M.; Schneider, J. F.; Tsuchida, J. E. Structural Characterization and Study of the Mixed-Ion Effect in K−Li Metaphosphate Glasses. *ACS Omega* **2025**, *10* (15), 15646−15653.
(66) Zeyer, M.; Montagne, L.; Kostoj, V.; Palavit, G.; Prochnow, D.; Jaeger, C. ^{17}O Nuclear Magnetic Resonance Study of Na_2O−P_2O_5 Glasses. *J. Non-Cryst. Solids* **2002**, *311* (3), 223−232.
(67) Muñoz, F.; Delevoye, L.; Montagne, L.; Charpentier, T. New Insights into the Structure of Oxynitride NaPON Phosphate Glasses by 17-Oxygen NMR. *J. Non-Cryst. Solids* **2013**, *363*, 134−139.
(68) Clark, T. M.; Grandinetti, P. J. Calculation of Bridging Oxygen Quadrupolar Coupling Parameters in Alkali Silicates: A Combined Ab Initio Investigation. *Solid State Nucl. Magn. Reson.* **2005**, *27* (4), 233−241.
(69) Clark, T. M.; Grandinetti, P. J.; Florian, P.; Stebbins, J. F. Correlated Structural Distributions in Silica Glass. *Phys. Rev. B* **2004**, *70* (6), No. 064202.
(70) Medek, A.; Harwood, J. S.; Frydman, L. Multiple-Quantum Magic-Angle Spinning NMR: A New Method for the Study of Quadrupolar Nuclei in Solids. *J. Am. Chem. Soc.* **1995**, *117* (51), 12779−12787.
(71) Swenson, J.; Matic, A.; Brodin, A.; Börjesson, L.; Howells, W. S. Structure of Mixed Alkali Phosphate Glasses by Neutron Diffraction and Raman Spectroscopy. *Phys. Rev. B* **1998**, *58* (17), No. 11331.
(72) Corbridge, D. E. C. The Crystal Structure of Rubidium Metaphosphate. *Acta Crystallogr.* **1956**, *9* (3), 308−314.
(73) Nord, A.; Lindberg, K.ChemInform Abstract: The Crystal Structure of Magnesium Tetrametaphosphate, $Mg_2P_4O_{12}$ *Chem. Informationsdienst* 1975; Vol. *6* .
(74) Turner, G. L.; Chung, S.; Oldfield, E. Solid-State Oxygen-17 Nuclear Magnetic Resonance Spectroscopic Study of the Group II Oxides. *J. Magn. Reson.* **1985**, *64* (2), 316−324.
(75) Sternberg, U. The Bond Angle Dependence of the Asymmetry Parameter of the Oxygen-17 Electric Field Gradient Tensor. *Solid State Nucl. Magn. Reson.* **1993**, *2* (4), 181−190.
(76) Liebau, F. The Influence of Cation Properties on the Conformation of Silicate and Phosphate Anions. In *Structure and Bonding in Crystals*; Academic Press: New York, 1981; Vol. *11*.
(77) Brown, I. D. Recent Developments in the Methods and Applications of the Bond Valence Model. *Chem. Rev.* **2009**, *109* (12), 6858−6919.
(78) Brown, I. D. The Bond-Valence Method: An Empirical Approach to Chemical Structure and Bonding. In *Industrial Chemistry Library*; Elsevier, 1981; Vol. *2*, pp 1−30.
(79) Yeo, T.-m.; Yuan, B.; Lovi, J.; Cho, J.-W.; Sen, S. Resolving the Mixed-Alkali Effect on the Viscoelastic Behavior of Supercooled Liquids. *Acta Mater.* **2023**, *242*, No. 118447.
(80) Day, D. E. Mixed Alkali Glasses-Their Properties and Uses. *J. Non-Cryst. Solids* **1976**, *21*, 343−372.
(81) Ingram, M. D.; Roling, B. The Concept of Matrix-Mediated Coupling: A New Interpretation of Mixed-Cation Effects in Glass. *J. Phys.: Condens. Matter* **2003**, *15* (16), S1595−S1605.
(82) Ingram, M. D. Ionic Conductivity and Glass Structure. *Philos. Mag. B* **1989**, *60* (6), 729−740.
(83) Maass, P.; Bunde, A.; Ingram, M. D. Ion Transport Anomalies in Glasses. *Phys. Rev. Lett.* **1992**, *68* (20), No. 3064.
(84) Jain, H.; Downing, H. L.; Peterson, N. L. The Mixed Alkali Effect in Lithium-Sodium Borate Glasses. *J. Non-Cryst. Solids* **1984**, *64* (3), 335−349.
(85) Chuang, S.; Yu, P.; Sen, S. Dynamic and Thermodynamic Behavior of Supercooled Na−Ba Metaphosphate Liquids: Role of Modifier Cation Ordering. *J. Am. Ceram. Soc.* **2025**, *108* (4), No. e20313.
(86) Shelby, J. E. Properties of Alkali−Alkaline Earth Metaphos-phate Glasses. *J. Non-Cryst. Solids* **2000**, *263*−*264*, 271−276.
(87) Wilder, J. A.; Shelby, J. E. Property Variation in Alkali Alkaline-Earth Metaphosphate Glasses. *J. Am. Ceram. Soc.* **1984**, *67* (6), 438−444.
(88) Yeo, T.-m.; Cho, J.-W.; Sen, S. Deciphering the Mixed-Alkali Effect in Supercooled Oxide Liquids: Results from Dynamic and Thermodynamic Measurements. *Acta Mater.* **2024**, *269*, No. 119798.

https://doi.org/10.1021/acs.jpcc.6c01260
J. Phys. Chem. C 2026, 130, 6243−6259